National Library of Canada

Cataloguing Branch
Canadian Theses Division

Ottawa, Canada
K1A 0N4

Bibliothèque nationale du Canada

Direction du catalogage
Division des thèses canadiennes

NOTICE

The quality of this microfiche is heavily dependent upon the quality of the original thesis submitted for microfilming. Every effort has been made to ensure the highest quality of reproduction possible.

If pages are missing, contact the university which granted the degree.

Some pages may have indistinct print especially if the original pages were typed with a poor typewriter ribbon or if the university sent us a poor photocopy.

Previously copyrighted materials (journal articles, published tests, etc.) are not filmed.

Reproduction in full or in part of this film is governed by the Canadian Copyright Act, R.S.C. 1970, c. C-30. Please read the authorization forms which accompany this thesis.

AVIS

La qualité de cette microfiche dépend grandement de la qualité de la thèse soumise au microfilmage. Nous avons tout fait pour assurer une qualité supérieure de reproduction.

S'il manque des pages, veuillez communiquer avec l'université qui a conféré le grade.

La qualité d'impression de certaines pages peut laisser à désirer, surtout si les pages originales ont été dactylographiées à l'aide d'un ruban usé ou si l'université nous a fait parvenir une photocopie de mauvaise qualité.

Les documents qui font déjà l'objet d'un droit d'auteur (articles de revue, examens publiés, etc.) ne sont pas microfilmés.

La reproduction, même partielle, de ce microfilm est soumise à la Loi canadienne sur le droit d'auteur, SRC 1970, c. C-30. Veuillez prendre connaissance des formules d'autorisation qui accompagnent cette thèse.

THIS DISSERTATION
HAS BEEN MICROFILMED
EXACTLY AS RECEIVED

LA THÈSE A ÉTÉ
MICROFILMÉE TELLE QUE
NOUS L'AVONS REÇUE

UNIVERSITÉ D'OTTAWA
UNIVERSITY OF OTTAWA

OXIDATION OF METHANOL OVER MOLYBDENUM OXIDE-TUNGSTEN OXIDE CATALYST

by

SATYENDRA KUMAR JAIN

A thesis submitted to the School of Graduate Studies
in partial fulfilment of the requirement for the degree of

MASTER OF APPLIED SCIENCE

in the

DEPARTMENT OF CHEMICAL ENGINEERING
UNIVERSITY OF OTTAWA

1976

ACKNOWLEDGEMENT

The author wishes to express his gratitude and sincere thanks to Professor R. S. Mann, for his advice, guidance, encouragement and unfailing interest during the course of this investigation.

The author is deeply indebted to Mr. M. K. Dosi, for his helpful suggestions and discussions, and to Mr. Denis Roy and Mr. G. Gasperatti for their technical assistance.

He is also greatful to Mrs. P. Serene, for typing the thesis and to Mr. R. K. Lal and Mr. Ashok Sahgal for their assistance from time to time.

TABLE OF CONTENTS

LIST OF TABLES

LIST OF FIGURES

ABSTRACT

The vapor phase oxidation of methanol to formaldehyde over molybdenum trioxide, tungsten trioxide and their mixtures has been investigated in an integral fixed bed tubular reacter, at atmospheric pressure. A preliminary study of the effects of the compositions of the mixed oxide catalyst on the yield of formaldehyde at 440°C indicated that maximum yield was obtained with a catalyst containing 45% Tungsten trioxide. A detailed kinetic study was made for methanol oxidation over 45% WO_3 - 55% MoO_3 catalyst.

The effect of various process variables namely, the concentration of methanol in feed, ratio of catalyst weight to methanol feed rate, and the process temperature on the conversion, selectivity and yield was determined.

The products were analyzed by a gas chromatograph and a gas partioner. Fifteen weight percent sucrose-octaacetate on colmpak T was used in the gas chromatograph for analyzing the liquid products, and hexamethylphosphoramide (HMPA) and molecular sieve 13X columns were used in the gas partioner for analyzing the gaseous products.

The tungsten trioxide - molybdenum trioxide catalyst was found to highly active for methanol oxidation. The maximum yield with 94.9% selectivity and 95.6% conversion was obtained at 426°C with a W/F ratio of 48.0 gm.-hr./mole. and 10 mole% methanol in air.

It was found that of several models proposed, only one correlated the data satisfactorily. This model has been derived on the basis of a two stage oxidation - reduction mechanism.

$$CH_3OH + s_{ox.} \xrightarrow{K_1} HCHO(g) + s_{red.}$$

$$O_2(g) + s_{red.} \xrightarrow{K_2} s_{ox.}$$

Where $s_{ox.}$ was an active site of lattice or adsorbed oxygen, and $s_{red.}$ was the reduced site of lattice oxygen or the empty site.

The rate of reaction was expressed by -

$$r = \frac{K_1 \cdot p_M}{1 + (K_1 \cdot p_M / 2 K_2 \cdot p_{O_2}^{0.5})}$$

Where K_1 and K_2 are temperature dependent rate constants.

I. INTRODUCTION

A. Importance of Chemical Kinetics

Chemical kinetics is a study of various factors which influence the rate of a chemical reaction. It is useful for gaining insight into the nature of a reaction system. It also helps in understanding how chemical bonds are broken and in estimating their energy and stability. It is important from the point of view of reactor design. Chemical kinetics is used in selecting the batch or continuous process, in finding the effect of concentration of reagents and operating conditions on the course of reaction. A correlation between the reaction rate and the process variables is important in obtaining optimum and economic process design.

In general, empirical rate expressions are sufficient for designing the equipment but true rate equations help in the extrapolation of the reaction conditions. It is important that reaction mechanism is studied for nearly actual operating plant conditions to make it more useful. High yield of desired product has to be kept in mind when studying the reaction from an industrial point of view.

B. Catalytic Reactions

Catalysis describes all processes in which the rate of reaction is influenced by the presence of a substance which remains chemically unaffected. Catalysts can increase the rate of thermodynamically feasible reactions only. A catalyst helps in increasing the rate of reaction because it provides an alternate mechanism, each step of which has a lower free energy of activation. This suggests that an intermediate substance might be formed by one or more of the reactants and the catalyst surface.

Catalytic reactions are classified according to whether they occur in single phase (homogeneous) or at an interface between two phases (heterogeneous). In the present investigation, oxidation of an oxygenated hydrocarbon catalyzed at a solid surface is studied.

C. Method of Study

A number of methods are available for measuring the reaction rate. Differential or integral reactors can be used in batch or continuous flow systems. The differential reactor is operated at small conversion. Reaction rate is assumed constant. Because of small conversion, it is generally difficult to analyze products precisely. In integral reactors, conversion is high, but it is difficult to integrate the rate expression because of a number of hidden parameters.

In the present investigation, a fixed bed integral flow reactor was used. Nearly atmospheric pressure was maintained. To obtain high yield, temperature was kept between 300°C to 500°C.

D. Objective of the Present Work

The purpose of the present investigation was to find a possible mechanism for the oxidation of methanol to formaldehyde over a mixture of Tungsten oxide and Molybdenum oxide catalyst. It was intended to develop a suitable rate expression which satisfactorily represented the data.

To obtain such a rate equation, it was desired to study the effect of various process variables on conversion, yield and selectivity.

II. LITERATURE SURVEY

Formaldehyde was discovered by the Russian chemist Buterov in 1859, as the product of attempted synthesis of methylene glycol. Hoffmann first prepared formaldehyde from methanol in 1890 and he established formaldehyde as the first member of the aldehyde group.

A comprehensive bibliography on formaldehyde research was published in 1964 by Walker as part of the American Chemical Society's monograph series[1]. A review of the literature on the oxidation of methanol has been written by Dosi[2] and Hahn[3]. The present survey is limited to literature on methanol oxidation over heterogeneous catalysts published after 1971. Various mechanisms proposed for similar reactions have also been reviewed.

A. Metal Catalysts

The principal method for producing formaldehyde presently used is oxidizing methanol over silver catalyst at a high temperature (500°C - 800°C). Effluent gases consist of 18-20% hydrogen, less than 1% oxygen and small amounts of carbon oxides and methane.

Kurina[4] has obtained a kinetic rate equation for methanol oxidation to formaldehyde. Diem Hans[5] obtained 88% yield and 98.5% conversion of methanol over silver catalyst. He used air washed with 4-20% methanol for the reaction. Obraztsov[7] studied methanol oxidation over silver catalyst. He observed that conversion of methanol increases while selectivity for formaldehyde production decreases as oxygen to methanol ratio is increased.

Several other catalysts have been tried for this particular reaction. They include zeolites containing transition metals[8], activated and dispersed phase metallic catalyst[9], lead tetraacetate[10] and alloy catalysts of Se or Sb with silver[11].

The reaction mechanisms proposed for the formation of formaldehyde are either a dehydrogenation, followed by the oxidation of hydrogen or a combination of dehydrogenation and oxidation reactions.

$$CH_3OH \rightleftharpoons HCHO + H_2 - 20 \text{ Kcals.} \qquad (2.1)$$

$$H_2 + 1/2O_2 \longrightarrow H_2O + 58 \text{ Kcals.} \qquad (2.2)$$

Proper control of the reaction temperature is important as pyrolytic decomposition of HCHO at higher temperatures increases significantly. The function of oxygen in the above reaction is to supply heat of reaction for first endo-thermic step and to oxidize and remove any substance from catalyst surface which poisons the catalyst.

B. Metal Oxide Catalysts

The use of metal oxide catalysts for methanol oxidation is achieving increasing importance in recent years. This process employed a metal oxide or mixtures of different metal oxides as a catalyst. It used feed gas containing methanol with a large excess of air and yielded a

formaldehyde product containing very little methanol in the product (0 - 1%). Reaction temperatures were generally in the range of 300°C - 500°C. The yield of formaldehyde by this process was much higher compared to that obtained by the use of a pure metal catalyst. The reaction takes place as

$$CH_3OH + 1/2O_2 \longrightarrow HCHO + H_2O + 38 \text{ Kcals.} \qquad (2.3)$$

Adkins[12] studied in detail methanol oxidation over iron oxide and molybdnum oxide catalysts. Molybdenum oxide catalyst was found to be highly selective though overall conversion was low. Iron oxide catalyst gave high conversion but converted nearly all methanol to carbon oxides. An equimolar mixture of these compounds was found to be suitable for obtaining a high yield of formaldehyde. Iron oxide and molybdenum oxide catalysts have been studied by various workers[13,14,15,16,17,21,22] recently. Phillipe[13] has reported a yield of 95.1 - 96.9% at 400 - 450°C. The use of 77 - 81% molybdenum oxide and remaining iron oxide at 380°C - 390°C yielded 95% selectivity and 94 - 99% conversion[15]. A critical review of Fe-Mo oxides catalyst has been published by Pernicone[18]. A yield of as high as 97% was reported by the use of 10 - 12% ferric oxide and remaining molybdenum trioxide[21].

Vanadium pentaoxide-chromium trioxide as catalyst was studied by Koval[19] and Popov[23]. Bliznakov[20] studied bismuth oxide-molybdenum trioxide as catalyst. Maximum activity was obtained for a catalyst containing $Bi_2O_3 \cdot 4MoO_3$. Selectivity increased up to MoO_3 - Bi_2O_3 ratio of 1:1, beyond which no change was observed. Tellurium-molybdenum oxides as catalyst have also been investigated[22]. These catalysts were not found suitable for obtaining a very high yield of formaldehyde.

C. Mechanisms and Rate Equations

Kowal[19] suggested that reaction mechanism depended on the composition of V_2O_5 - Cr_2O_3 catalyst. The activity of the catalyst increased with the decrease in the strength of the oxygen bond on the catalyst surface. Oxides in which an exchange of lattice oxygen with O_2(gas) was slow, were found to be more selective.

Jiru[24,25] studied rate mechanism for the oxidation of methanol over 17.5% Fe_2O_3 - 82.5% MoO_3. They deduced a rate expression based on a mechanism originally proposed by Mars and Krevelen for vapor phase oxidation of aromatic hydrocarbons on vanadium pentaoxide as catalyst. The mechanism proposed by Mars was -

$$\text{Reactant} + \text{Catalyst}_{ox.} \longrightarrow \text{Product} + \text{Catalyst}_{Red.} \qquad (2.4)$$

$$\text{Catalyst}_{Red.} + O_2 \longrightarrow \text{Catalyst}_{ox.} \qquad (2.5)$$

The rate expression obtained by Jiru was -

$$r = \frac{K_1 P_M^m}{1 + K_1 P_M^m / K_2 P_{O_2}^n} \qquad (2.6)$$

m and n were found to be equal to 1 and 0.5 respectively. A similar rate expression was also obtained by Dente[27,28].

Klissurski[29] claimed that the oxidation of methanol takes place by the removal of surface or lattice oxygen followed by adsorption of O from the gas phase. The rate of reaction depended on the stability of the bond between O and surface layer of the catalyst. Gresmundo[37] carried out ESR studies on MoO_3, V_2O_5, Cr_2O_3 to find out as to how these catalysts were modified during the oxidation of methanol. He concluded that O atoms of the catalyst took part in the reaction. The catalyst was

reduced by CH_3OH followed by its consequent oxidation by molecular oxygen.

Using a microcatalytic pulse technique, Jiru[24] observed the rate of oxidation of methanol at 270°C over Fe_2O_3 - MoO_3 catalyst. He first determined the rate of interaction between methanol and the catalyst without participation of air and then determined the rate of interaction between oxygen and a partially reduced catalyst without the participation of methanol. He observed a remarkable equality between the amount of oxygen removed by methanol and oxygen subsequently taken up by the catalyst. It was concluded that the lattice oxygen of the oxide catalyst participated in the oxidation process. He also observed a change in the color of the catalyst from yellowish green to greyish blue during the course of reaction. He suggested color change might be because of change in the valency caused by the loss of lattice oxygen.

Mars and Krevelen[26] studied the oxidation of several aromatic hydrocarbons over vanadium pentaoxide. He observed a change in the color of catalyst from yellowish brown in the oxidized state to greenish blue in the reduced state. This color change was reversible. When the catalyst was analyzed in the reduced state, a high concentration of tetravalent vanadium was found. V_2O_5 has three fifths of oxygen existing in the same plane as vanadium, while two fifths of oxygen is arranged in planes parallel to and alternating with the first. They suggested that alternating lattice oxygen interacted with aromatic molecules at the surface of the catalyst. Bhattacharya[52] studied the oxidation of methanol over vanadium pentaoxide catalyst and observed a similar reaction mechanism. Dosi[2] and Hahn[3] reported a similar two stage redox mechanism for methanol oxidation over V_2O_5 - MoO_3 and MnO_2 - MoO_3 catalysts. Hahn observed a change in the color of the catalyst which was not reversible. This phenomenon could not be explained by him.

Shelstad[53, 54] studied oxidation of napthalene and toluene. They also observed a two stage redox mechanism, however, they suggested that oxygen physically adsorbed on the catalyst surface reacts with other reactants in the gaseous phase. The rate of the removal of oxygen adsorbed on the catalyst surface equals the amount of oxygen being adsorbed on the catalyst. Ioffe[55] also favoured this mechanism.

Tarama[56] studied x-ray diffraction of V-O bond in V_2O_5. He observed that the V-O bond was weak and similar to a double bond. This bond was further weakened when MoO_3 was added as it formed a solid solution with V_2O_5. Hence, it is quite possible that lattice oxygen takes part in the reaction catalyzed by similar catalysts.

Bennet[30] and Cotter[31] studied the kinetics of methanol oxidation and suggested the rate expression

$$r = K p_M^m \qquad (2.7)$$

Bennet used a flow recycling differential bed reactor between 402°C-452°C and a lean methanol-air mixture (up to 3% methanol). Cotter used a fixed bed integral reactor between 260°C - 330°C, methanol concentration of 1-3 mole % and a gas flow rate of up to 0.9 cuft./min. Jiru[32] also studied kinetics in a differential reactor with recycle at 370°C and obtained a rate equation with $m = 1$ and $n = 0.5$.

Boreskov[33] investigated the nature and phase of iron-molybdenum oxide catalyst by means of x-ray, EPR, infrared and thermographic analysis. Normal iron molybdate proved to be the active component. Popov[34] reported active components of a similar catalyst to be consisting of Mo_1-O-Mo_2 and Mo_1-O-Fe-O-Mo_2. Alexe Szabo[38] observed that formaldehyde yield increased by 25% when 5.52% Fe_2O_3 was added to Mo-Bi oxide catalysts. He suggested that bismuth molybdate, iron molybdate and molybdenum trioxide were active components in catalyst.

D. Tungsten Oxide as a Catalyst for Methanol Oxidation

Bliznakov[35] studied the catalytic action of tungstates of period IV metals. All tungstates studied showed medium catalytic activity, the highest being for iron tungstate.

Arnold[36] patented a method of the preparation for molybdenum-tungsten oxide catalysts. He also studied methanol oxidation over different compositions of catalysts. He obtained a very high yield of formaldehyde.

Popov[39] studied the catalytic activity of tungsten trioxide with molybdenum trioxide and manganese dioxide during the oxidation of methanol. The degree of oxidation increased to ~6% with increasing temperature. Conversion was 70% at 450°C, when the ratio of MnO_2 and WO_3 was 1:2. X-ray analysis showed $MnWO_4$ to be active centres. Popov[40] also reported results for methanol oxidation at varying compositions of bismuth oxide and tungsten oxide in the range of 250°C - 450°C.

Liminov[41] studied the effect of catalyst composition for WO_3 and MoO_3 mixtures. The x-ray analysis of the catalyst showed peaks corresponding to $MoO_3 \cdot WO_3$ mixture. They studied the effect of catalyst composition and temperature, on the conversion and the selectivity, in the temperature range of 300°C - 450°C. The selectivity of the reaction for formaldehyde increased with the percentage of MoO_3 in the catalyst with a point of inflection between 38% - 50% MoO_3. Conversion decreased with an increase of molybdenum trioxide in the catalyst. Optimum proportion of catalyst for maximum yield was within the range MoO_3(46-56%) and WO_3 (44-54%).

There has been no attempt made so far to study in detail the kinetics of the oxidation of methanol over molybdenum oxide-tungsten oxide catalyst.

III THEORY OF KINETIC ANALYSIS OF DATA

Determination of the relationship between reaction rate and operating variables is an important step in the design of any catalytic process. It is generally accepted to derive a rate expression in terms of partial pressures based on the Langmuir Hinshelwood Theory[42].

A. Various steps in heterogeneous catalytic reaction

The starting point for studying the kinetics is to study the sequence of physical and chemical steps which occur in the heterogeneous reaction. Various steps are -

1. Transport of reactants from the bulk fluid phase to the solid fluid interface.
2. Internal diffusion of the reactants along the pores.
3. Adsorption of the reactants on the solid surface.
4. A surface reaction between an adsorbed reactant on the catalyst surface and either one of the gaseous reactants or other adsorbed reactants on the surface.
5. Desorption of the products from the surface to fluid-solid interface.

6. Internal diffusion of products along the pores to the outer surface.
7. Transport of products from interface to the bulk fluid stream.

In case resistance offered by each of these steps is considered, the rate expression would be very complicated. The importance of the various steps vary greatly, depending upon operating conditions. Steps 1, 2, 6, 7 being physical processes, can be minimized or eliminated by making catalyst centres easily accessible and by having high turbulent flow. Chemical steps 2, 3, 4 offer much higher resistances. In most of the cases, only one of these steps is rate controlling.

B. Various Correlations of Rate Equations

1. Langmuir Hinshelwood mechanism:

This theory, based on the concept of monolayer chemisorption on the surface of catalyst, assumes adsorption and desorption processes to be in equilibrium at constant temperature. This mechanism assumes that reaction takes place between either (a) an adsorbed molecule and a gaseous reactant molecule, or (b) two chemisorbed molecules on adjacent sites.

Rate equation is derived by assuming a rate mechanism and selecting one of the reaction steps as rate controlling. The slowest steps control the reaction. For a bimolecular reaction, the rate expression has been developed by Smith[43]. Other rate equations have been systematically developed and compiled by Hougen and Watson[44] and by Yang and Hougen[45] for various reaction mechanisms with different rate controlling steps.

The details of this particular mechanism are reviewed by Hahn[3]. This mechanism is not favoured for oxygenated hydrocarbons.

2. Modified Langmuir - Hinshelwood Mechanisms :

When the rate of adsorption of reactants offers significant resistance, the assumption of adsorption equilibrium in the Langmuir Hinshelwood theory is not valid. The modified theory considers that reactant adsorbed on the surface increases by adsorption and decreases by reaction. The stationary conditions are established when the two rates are equal.

Oxidation of oxygenated hydrocarbons can be treated as an irreversible two or three stage oxidation-reduction reaction. The mechanisms following this are generally referred to as "Redox mechanisms". Two stage redox mechanism is considered in detail here. Three stage redox mechanism has been reviewed by Hahn[3].

Two Stage Redox Mechanism.

According to this mechanism, a steady state is assumed between the following two steps with the equilibrium shifted to the right side.

$$m\,[\,CH_3OH + S_{ox} \xrightarrow{K_1} HCHO(g) + H_2O + S_{red.}\,] \qquad (3.1)$$

$$n\,[\,O_2(g) + S_{red.} \xrightarrow{K_2} S_{ox.}\,] \qquad (3.2)$$

The rates of reaction for two cases are :

$$r_1 = K_1 p_M^m \theta \qquad (3.3)$$

$$r_2 = K_2 p_{O_2}^n (1 - \theta) \qquad (3.4)$$

$$\propto r_1 = r_2 \qquad (3.5)$$

θ is defined as a fraction of catalyst surface covered by adsorbed or lattice oxygen and α is the number of oxygen molecules required to convert one molecule of methanol, that is 0.5 in the present case. Based on 3.3, 3.4 and 3.5, the following relations are derived :

$$\theta = 1/(1 + \alpha K_1 p_M^m / K_2 p_{O_2}^n) \qquad (3.6)$$

$$r = r_1 = K_1 p_M^m / (1 + \alpha K_1 p_M^m / K_2 p_{O_2}^n) \qquad (3.7)$$

r is the rate of oxidation of methanol to formaldehyde. The integrated forms of rate equations with different m and n values are listed in table 3.1. Different terms used in table 3.1 are :

$$p_M = {}^o p_M (1 - x)$$

$$p_{O_2} = {}^o p_{O_2} - 1/2 \cdot {}^o p_M \cdot x ,$$

p_M = Partial pressure of methanol at time t.

${}^o p_M$ = Partial pressure of methanol in the feed.

p_{O_2} = Partial pressure of oxygen at time t.

${}^o p_{O_2}$ = Partial pressure of oxygen in the feed.

x = Percentage conversion.

As explained earlier in Chapter II, the two stage redox mechanism is reported to be suitable for the kinetic study of methanol oxidation over catalyst similar to WO_3 - MoO_3.

Table 3-I

Two-Stage Redox Mechanisms

No	Reaction Order m CH_3OH	Reaction Order n O_2	Integrated Rate Equation
1	1	0.5	$\frac{W}{F}\frac{{}_oP_M}{\ln(1-x)} = -\frac{1}{k_1} + \frac{4\alpha}{k_2}\left(\frac{\left[{}_oP_{O_2}^{\frac{1}{2}} - \left({}_oP_{O_2} - \frac{1}{2}x\,{}_oP_M\right)^{\frac{1}{2}}\right]}{\ln(1-x)}\right)$
2	1	0	$\frac{W}{F}\frac{1}{x} = -\frac{1}{k_1}\frac{\ln(1-x)}{{}_oP_M x} + \frac{\alpha}{k_2}$
3	0.5	0	$\frac{W}{F}\frac{1}{x} = \frac{2}{k_1}\frac{\left[1-(1-x)^{\frac{1}{2}}\right]}{{}_oP_M^{\frac{1}{2}} x} + \frac{\alpha}{k_2}$
4	1	1	$\frac{W}{F}\frac{{}_oP_M}{\ln(1-x)} = -\frac{1}{k_1} + \frac{2\alpha}{k_2}\frac{\ln\left[{}_oP_{O_2}/\left({}_oP_{O_2} - \frac{1}{2}\,{}_oP_M x\right)\right]}{\ln(1-x)}$
5	0.5	0.5	$\frac{W}{F}\frac{{}_oP_M^{\frac{1}{2}}}{\left[1-(1-x)^{\frac{1}{2}}\right]} = \frac{2}{k_1} + \frac{4\alpha}{k_2}\cdot\frac{{}_oP_{O_2}^{\frac{1}{2}} - \left({}_oP_{O_2} - \frac{1}{2}\,{}_oP_M x\right)^{\frac{1}{2}}}{{}_oP_M^{\frac{1}{2}}\left[1-(1-x)^{\frac{1}{2}}\right]}$

IV. EXPERIMENTAL DESCRIPTION

A. Apparatus

A schematic diagram of apparatus used is shown in fig. 4. 1.

Two Helium gas streams are supplied as carrier gas to the gas chromatograph and gas partitioner. The third stream carrying calibrating gas (CO, CO_2, N_2) and fourth stream carrying air were used to prepare gaseous mixtures for calibration. The fourth stream was also connected to the hot inlet and was used for preparing feed mixtures with vaporised methanol. Another air stream was used for fluidizing the sand bed in the reactor assembly.

Calibrating gases, air and Helium, were supplied from high pressure cylinders through two stage pressure regulators (Model 8, Matheson of Canada Ltd., Whitby, Ontario). Traces of moisture in the air were removed by passing it through a drying tube packed with "drierite". Gas lines were made of 1/8" OD copper tubing. Gas lines coming out from rotameters and beyond that, in stream three and four were made of 1/8" OD stainless steel tubing. Fine metering valves and unidirectional check valves (Nupro Co., Cleveland, Ohio) were used. All other fittings were made by (Crawford Fittings Company, Cleveland, Ohio).

Figure 4-1 Diagram of Experimental Apparatus

Symbol	Item
AS	Air Supply unit
C	Water Condenser
CG	Calibrating gas cylinder
D_1, D_2	Drying tubes
GC	Gas Chromatograph
GP	Gas Partitioner
HI	Hot Inlet
LT	Liquid Trap
P	Pressure Gauges
R_1, R_2, R_3, R_4	Rotameters
R	Chart Recorder
SP	Syringe Pump
SV	Sample Valve
TC	Temperature Controller
W	Wet Test Meter
ZS	Zero Suppressor

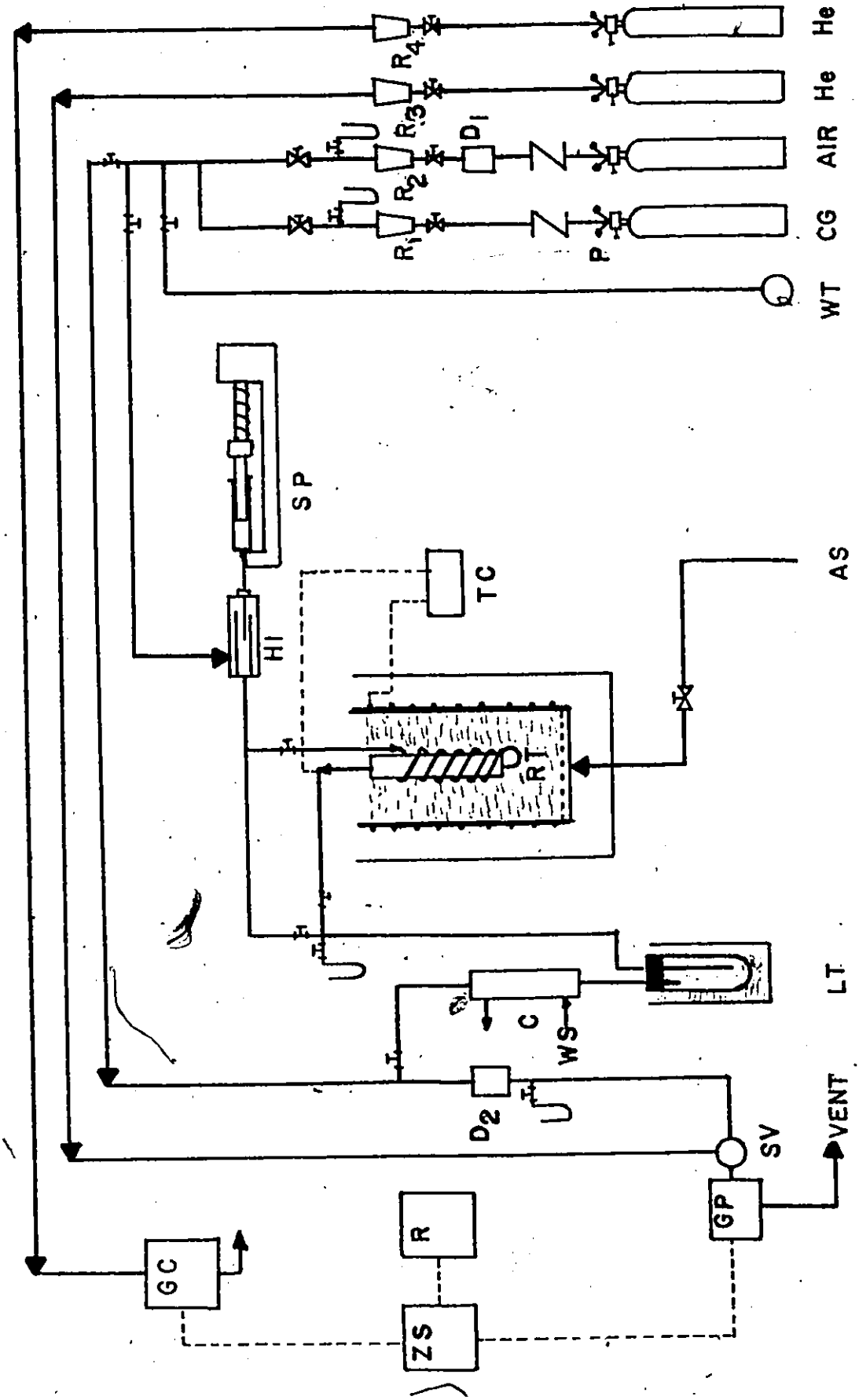

Fig. 4.1 Schematic Diagram of Experimental Apparatus

Flow rates of each gas stream were measured by rotameters (body) series 622 PSV and 622 BSI, flowmeter tube and float series 601 and 602 Matheson of Canada Ltd., Whitby, Ontario). To reduce the pressure effect on flow rates, rotameters for calibrating gas and air were connected with mercury manometers.

To infuse methanol in the feed stream, an infusion syringe pump (Model 901, Harvard Apparatus Co., Inc., Millis, Mass.) and 10 cc gas tight syringe (#1010 Hamilton Co., Reno, Nevada) was used. Methanol was injected into a hot inlet (Model 86800 Hamilton Co., Whitby, Cal.), through which the air stream was passed at high velocity. Methanol was continuously vaporised and carried away in an air stream. Stainless steel tubing carrying the air and methanol mixture to the reactor was continuously heated externally by heating tape (Cat. No. HT344, Electrothermal Engg. Ltd., London, England).

The reactant stream coming out of the hot inlet could either be bypassed to the liquid trap or could be sent to the preheater and reactor. The feed stream going to the reactor was preheated in 8' x 1/8" OD stainless steel tubing wound around the reactor. The stream was passed into the reactor through the bottom. The reactor was 7 1/2" x 0.39" ID stainless steel tube. A porous stainless steel plate was fixed at the bottom of the reactor. The top of the reactor was connected by a reducer to 5/4" x 1/4" OD stainless steel tube. This was further connected to a Swaglok "T" connection (810-3-2-316). One end of the "T" was connected to a 1/8" OD stainless steel tubing through a reducer. Through the other end of the "T", a 1/8" OD stainless steel tube containing iron constantan thermocouple was inserted. The lower end of the thermocouple was kept just above the porous plate. The thermocouple was connected to the temperature controller (Honeywell C-FI-84855-001). The thermocouple could be connected to a millivolt potentiometer (James G. Biddle Co., Plymouth Meeting, Pa., Cat. 72-310, Ser. 46811) for measuring the exact temperature.

The reactor and preheater were kept immersed in a constant temperature fluidized bed furnace. The container for the fluidized sand bed was a 4 1/2" OD steel cylinder. A porous stainless steel plate was welded at the bottom. This cylinder was connected to the departmental air supply. Air, passing through the sand bed could be regulated by a metering valve. The reactor was held straight in the sand bed. Sufficient air was passed to keep the sand fluidized and to obtain a uniform temperature around the reactor. For heating the fluidized bed, ceram -A- Flex beaded heating wires were wrapped around the cylinder. These heating wires were connected to a ten amp. powerstat (Type 116B, Superior Electric Co., Bristol, Conn.) through a temperature controller placed in series. The temperature in the sand bed was adjusted by changing the input voltage using a powerstat. The reactor and the fluidized sand bed were placed in a 12" OD cylinder. The annular space was filled with insulation. The heating tape and hot inlet were also supplied power through two 7 1/2 amp. voltage regulators.

Products coming out of the reactor were passed through a 1/8" OD stainless steel tube heated externally. Products were passed through a liquid trap made of a 7 1/2" x 7/8" OD glass tube, fitted with a two-hole rubber stopper. This tube was placed in a dewarflask filled with a mixture of ice and sodium chloride. Heavier products, formaldehyde, water and methanol continuously condensed in the liquid trap. Uncondensed gases were passed through a 1/8" OD tube placed in a 10 1/2" x 3 1/2" OD cylinder. Through this cylinder, fresh cold water continuously passed to cool the products passing through the tube. Any products condensing in the inside tube dropped back into the liquid trap. Products coming out of the condenser were passed through a trying tube made of 5 1/2" x 2 1/2" OD acrylic tube filled with drierite. All traces of moisture from the gaseous products were removed in the drying tube and condenser.

The gaseous products were then passed through a fisher gas partitioner (Model 25V) through a linear sampling valve. A stream of helium was also

passed through a sample loop and then vented to atmosphere. When the sample loop was turned on, the sampling valve was taken out of the product stream and connected with the carrier gas stream. The temperature inside the partitioner was controlled by a Fisher's thermal stabilizer (Model 27). The signal from the gas partitioner was transferred through a zero suppressor (Model 23, Fisher Scientific Co.) to a chart recorder (Electronik 19, 19-4112-003-003-01, Honeywell, Ft. Washington Pa.).

Liquid samples were analyzed by injecting them through a 10$\mu\ell$ gas tight syringe (#701 N or #801 N, Hamilton Co., Reno, Nevada) into a gas chromatograph (Varian Aerograph A-90-P3). The chromatograph was connected to the same chart recorder.

B. Reactants and Chemicals

The following chemicals were used during the course of the present investigation:

1. Methanol - Certified A. C. S. spectroanalyzed methanol (Cat. No. A-408, Lot No. 743404, Fisher Scientific Co.)
2. Formaldehyde Solution - Baker Analyzed Reagent (Cat. No. 2106, Lot No. 44466, J. T. Baker Chemical Co., Phillipsburg, N. J.)
3. Indicating Drierite - 8 mesh (W. A. Hammond Drierite Co., Xenia, Ohio)
4. Ammonium paratungstate $(NH_4)_6\ W_7O_{24} \cdot 6H_2O$ - (Cat. No. 4104, ICN Pharmaceuticals Inc., Life Science Group, Plainview, N. Y.)
5. Ammonium molybdate $(NH_4)_6\ Mo_7O_{24} \cdot 4H_2O$ - (Cat. No. 0716, J. T. Baker Chemicals Co., Phillipsburg, N. J.)
6. Compressed Air Cylinders - (Liquid Carbonic of Canada, Ltd.)

7. Helium gas cylinders - (Linde Helium, Union Carbide of Canada Ltd., Whitby, Ontario)
8. Compressed Carbon dioxide and Carbon monoxide cylinder - (Matheson of Canada Ltd., Whitby, Ontario)
9. 30% Hexamethylene phosphormide on 60-80 mesh Columpak - (11-130-57, Fisher Scientific Co.)
10. Molecular Sieve 13X - Chromatograph Grade, 42/60 mesh (Lot No. 112469, Coast Engineering Lab.)
11. Golumpak T - 40/60 mesh (Cat. No. C-587, Fisher Scientific Co.)
12. Compressed Nitrogen Cylinders - (Linde, Union Carbide of Canada, Ltd.)

C. Preparation and Properties of Catalyst

(i) Molybdenum Trioxide and Tungsten Trioxide -

Pure molybdenum trioxide and tungsten trioxide catalysts were obtained by the thermal decomposition of ammonium molybdate and ammonium paratungstate. These compounds were heated for 6 hours at 150°C and for 2 hours each at 200°C, 300°C and 400°C. The catalysts were calcined for 6 hours at 500°C and activated for 2 hours at 600°C.

(ii) Molybdenum Trioxide - Tungsten Trioxide Mixtures -

Ammonium molybdate and ammonium paratungstate were weighed according to the desired ratio of molybdenum trioxide and tungsten trioxide. Ammonium molybdate was dissolved in distilled water. Ammonium paratungstate was added to this solution and heated at a low temperature. The solution was continuously stirred until all ammonium paratungstate dissolved. This solution was then heated at a low temperature to obtain a paste. The paste was dried for 12 hours at 40°F. Further heat treatment was similar to that for pure catalysts.

60/80 mesh size catalyst particles were used for all experimental runs. Surface area of catalyst as determined by the BET method for 45% WO_3 catalyst was 1.31 m^2/gm.

All catalysts were reactivated at 500°C for 8-12 hours in the reactor before starting the experiments. The catalyst had a light green color.

D. Experimental Procedure

1. Calibration : ⟶ Flow rates of different gas streams were measured by the rotameters, which were precalibrated. The rotameters were calibrated by measuring the flow rates by a wet test meter (Precision Scientific Co., Chicago). Pressure at the outlet of the rotameter was maintained constant. Rotameters were calibrated for Air, CO, CO_2 and N_2. The calibration curve for air is given in Appendix 8-C.

Liquid flow rates of methanol could be controlled by using different speeds of pump and using different syringe sizes. For a particular condition used in all the experiments, the feed rate was calibrated by pumping methanol for some interval of time. The rate of methanol infusion thus calculated, matched with that specified for the pump.

Thermocouples used were checked by inserting them in a fluidized sand bath, measuring millivoltage by the potentiometer and checking the temperature with a thermometer (Cat. No. 14-985H, Fisher Scientific). The temperature obtained by reading charts for iron constanton thermocouple matched perfectly with the temperatures obtained by the thermometer.

For the calibration of the gas partitioner and gas chromatograph, synthetic gas and liquid mixtures were made. Mixtures of carbon dioxide, carbon monoxide and nitrogen were made with air in varying proportions and separated by gas partitioner. Mixtures of water, methanol and formaldehyde were injected into the chromatograph. Calibration curves for one

chromatograph column and gas partitioner are shown in Appendix 8-C. The calibration of this equipment was repeatedly checked by injecting standard samples in between different runs.

2. Analysis Procedure : ⟶ To analyze the gaseous products containing CO, CO_2, N_2 and O_2, two columns were used in the gas partitioner. The first column was 5'6"x1/4" OD copper tubing, packed with 30% HMPA coated on columpak. This column could separate carbon dioxide. The column was followed by 18' x 3/8" OD copper tubing packed with molecular sieve 13X. Conditions in the gas partitioner as well as in the chromatograph are given in Appendix 8-C. A typical analysis of the gas mixture is given in figure 4.2 .

For analyzing the liquid products, a 15' x 1/4" OD copper tubing column packed with 15 wt. % sucrose octaacetate coated on columpak T (40-60 mesh) was obtained from "Chromatography Specialists Ltd., Brockville, Ontario". This column was stabilized by heating for one hour prior to its use at 190°C. A typical analysis of liquid products is shown in figure 4.3. The liquid samples were analyzed immediately at the end of each run to avoid possible polymerization of formaldehyde.

3. Leakage : ⟶ The system was checked for possible leakage as follows -

(i) Every connection was tested with "snoop" after closing the down stream valves and maintaining a pressure of 30 psig in the system.

(ii) Under the above conditions, there was no indication of air flowing through the system.

(iii) After maintaining a pressure of 30 psig in the system, the air supply was closed. There was no indication of a pressure drop after a couple of hours.

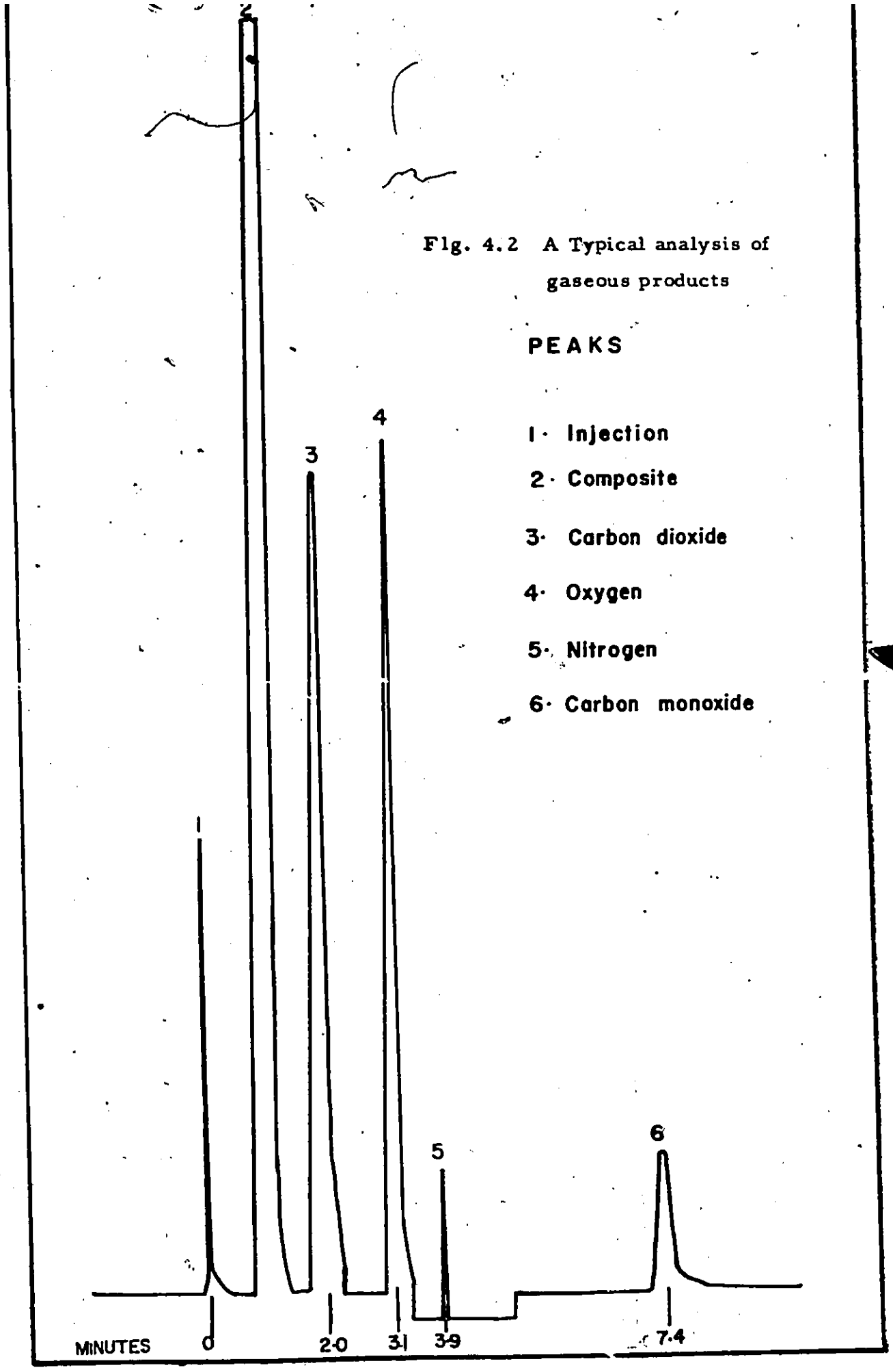

Flg. 4.2 A Typical analysis of gaseous products

PEAKS

1· Injection

2· Composite

3· Carbon dioxide

4· Oxygen

5· Nitrogen

6· Carbon monoxide

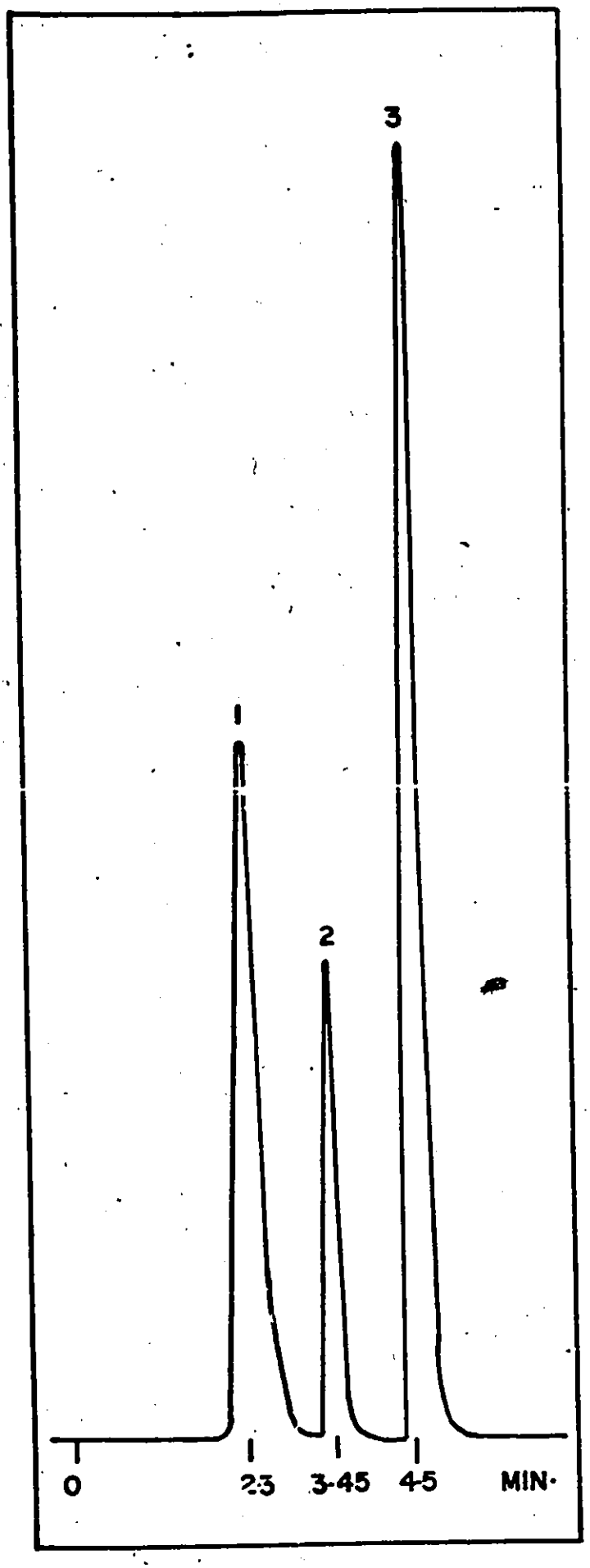

Figure 4.3

A typical analysis of Liquid Products

PEAKS

(1) Formaldehyde

(2) Methanol

(3) Water

4. Operating Procedures : ⟶

(i) Check the system for possible leakage.

(ii) Place a weighed amount of the catalyst in the reactor. Cover the reactor with glass wool. Place the thermocouple assembly on top of the reactor and reassemble the reactor.

(iii) Clamp the reactor placing it upright in the fluidized bed. Cover the top of the furnace with asbestos sheets to prevent outflow of sand. Connect the reactor to the incoming air line and outgoing product line.

(iv) Turn on the air stream. Check for possible leaks.

(v) Turn on the power to the reactor. Adjust powerstat voltage and air flow rate to the fluidized bed so as to obtain the desired temperature. Temperature was initially raised to 500°C for the activation of the catalyst. Approximately 48 hours are required for obtaining the exact temperature and to reach an equilibrium.

(vi) Switch on the power to the hot inlet and heating tape.

(vii) Switch on the power to the gas partitioner and gas chromatograph and set the required conditions. After the start up, power to the chromatograph and the partitioner are left on and helium is continuously supplied to the system.

(viii) After the set conditions have been achieved, switch on the recorder and check that the base lines are straight.

(ix) Place the liquid trap in position. Fill a dewar flask with freezing mixture. Turn on the water supply for the condenser.

(xi) Adjust the air flow rate in the rotameter. At intervals, air flow rate is checked by wet test meter. The air flow is adjusted to give constant molar flow rate required.

(xii) Switch on the infusion pump and start feeding methanol. Methanol and air are fed to the system for 2 hours or more to see

that the system remains at a steady state. Steady state conditions are checked by analyzing the gas products and checking the temperature in the reactor.

(xiii) Replace the clean dry tube in the dewar flask. Collect the samples for nearly one hour. During this time, gas products are repeatedly analyzed.

(xiv) Analyze the liquid sample after removing the liquid samples from the tube into a sample bottle.

(xv) Shut off the methanol feed pump. Air is allowed to flow through the system for a couple of hours before making the next run.

(xvi) System is again allowed to stabilize by adjusting the powerstat and leaving it to stabilize overnight.

(xvii) As mentioned earlier, it is important to check the columns periodically by checking the calibration of the chromatograph and partitioner.

V RESULTS

A. Preliminary Studies

The experimental data was obtained to study the effect of (a) composition of the catalyst keeping all other process variables constant, (b) temperature, T , (c) concentration of methanol in feed mixture, R , (d) ratio of catalyst weight to methanol feed rate, W/F.

Conversion is defined as the ratio of moles of methanol reacted to moles of methanol fed per unit time. Yield is defined as the ratio of formaldehyde formed to methanol fed per unit time. Selectivity is the ratio of formaldehyde formed to the sum of formaldehyde, carbon dioxide, carbon monoxide formed per unit time.

Methanol feed rate was kept constant for all the runs. The methanol concentration in the feed was varied by changing the amount of air. W/F was varied by changing the amount of the catalyst in the reactor.

Figure 5.1 shows the effect of the catalyst composition on conversion, selectivity and yield. Experimental data is listed in Appendix 8-A.

Based on this curve and other available data in the literature, 45% WO_3 - 55% MoO_3 was considered suitable for detailed kinetic studies.

B. Kinetic Analysis of Data

1. Factors affecting rate mechanism - The rate equation is generally derived in terms of temperature, pressure and composition of the reactants. The other factors which might affect kinetics are considered below :-

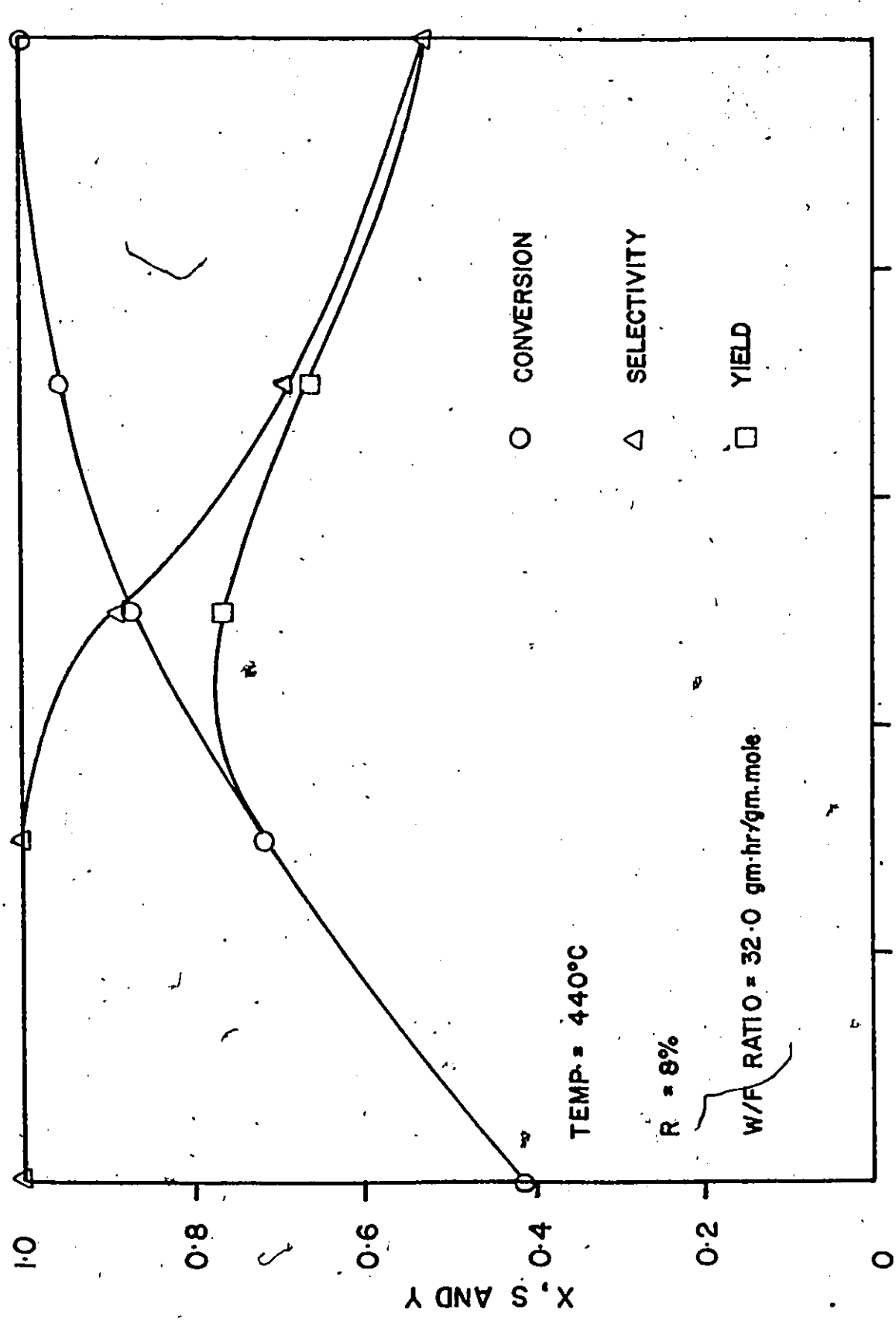

Figure 5.1 Effect of Catalyst composition

I. Activity of Catalyst - Catalytic activity remained fairly constant over all the runs for a particular catalyst. This was confirmed by repeating the initial run after all runs had been taken for the catalyst.

II. Homogeneous reactions and reactions in the absence of catalyst - No reaction was observed between methanol and air at 470°C in the absence of catalyst.

III. Side Reactions - Formation of carbon monoxide is believed to be caused by the thermal decomposition of formaldehyde. Carbon dioxide is formed by the oxidation of carbon monoxide. This particular factor is assumed and the effect of side reactions is not taken into account. As observed in most of the experimental data, the amount of carbon oxides formed was quite small compared to the total products. For correlation of data, total conversion is used as the amount of formaldehyde produced. Experimental runs where carbon oxides formed were more than 5% of total products were not considered for kinetic analysis.

IV. Pressure drop through catalyst bed - Total pressure inside the reactor was measured in the absence of catalyst. Since pressure drop did not exceed 15 mm of Hg when the catalyst was present, constant total pressure was assumed in all the runs. Pressure at the outlet of reactor (866.0 mm of Hg) was taken as total pressure in catalyst bed.

V. Departure from plug flow - In the present study, flat velocity profile (plug flow) in the reactor tube was assumed. The flat pattern in the tube is affected by a number of factors. Smith [46, 47] observed that deviation from uniform velocity profile is very insignificant if the ratio of tube to pellet diameter is greater than 30. The ratio of tube to pellet diameter is more that 41 in the present work. Hence, the assumption of plug flow did not result in any significant error.

VI. Internal diffusion - Internal diffusion can be of two kinds:

(a) Molecular diffusion - When the mean free path of diffusing molecules is small with respect to pore radius, collisions between molecules of reactants control the diffusion process. This is known as molecular diffusion or bulk diffusion. In such cases, the partial pressure of the different reactants control the diffusion process. In most of the cases, this type of diffusion is insignificant unless pressure is very high or pore radii is very large.

Present work was conducted at nearly atmospheric pressure. Molecular diffusion is expected to be negligible.

To check the effect of molecular diffusion, two runs were taken at the same conditions. The feed velocity of methanol was varied. Changing feed velocity had no effect on conversion. Results are shown in Appendix 8-E. Hence, it can be assumed that molecular diffusion did not control the reaction.

(b) Knudson diffusion - In most of the catalysts, Knudson diffusion offers much larger resistance to diffusion process. When pore size of catalyst is small, collisions between molecules and pore wall control the diffusion process. In general, conditions existing inside pores may be considerably different from those existing outside the surface of catalyst. It has not been possible to correlate the effect due to Knudson diffusion with physical properties of catalyst. The catalyst particles used in the present study were 60/80 mesh size. For such small catalyst particles, Knudson diffusion does not effect results significantly.

To find if Knudson diffusion affected the results, two runs were taken at the same conditions but changing particle diameter. Conversion was nearly the same. Results are shown in Appendix 8-E. In case Knudson diffusion was affecting the results significantly, changing catalyst diameter should have resulted in significant change in the rate of reaction. Hence, it can be assumed that Knudson diffusion effects were negligible.

The diffusion of any kind was negligible because feed velocity through catalyst bed was very high.

VII. Resistance to external heat and mass transfer - The values of partial pressure and temperature in the bulk stream and at the gas solid interface may differ significantly in certain systems. However, to simplify the correlation for experimental data, it is necessary to minimize these resistances so that they are negligible. The effect of heat and mass transfer can be seen from the following relations :

$$r_{MA} = k_{GA} a_M \varphi (P_A - P_{Ai}) \qquad (5.1)$$

$$g_{MA} = r_{MA} \Delta H_A - h_G a_M \varphi (T - T_i) \qquad (5.2)$$

where

r_{MA} = rate of reaction or mass transfer of A per unit mass of catalyst.

g_{MA} = heat transfer due to heat of reaction per unit mass of catalyst.

k_{GA} = mass transfer coefficient for component A.

h_G = heat transfer coefficient per unit exterior surface of catalyst particle.

a_M = external surface area of catalyst per unit mass.

φ = shape factor

P_A = partial pressure of component A in the ambient stream.

P_{Ai} = partial pressure of component A at the catalyst surface.

T = temperature of the ambient stream.

T_i = temperature of the catalyst.

The transfer coefficients can be calculated by the dimensionless Chilton Colburn j factors[48]. The j factors can be calculated from expressions developed by Gausson, Thodes and Hougan[49] and by Wilke and Hougen[50] in different ranges of Reynold number.

The mathematical procedure for calculating the temperature and the partial pressure at the surface of the catalyst particles for flow reactions in fixed beds has been developed by Yoshida et al.[51].

The temperature drop and partial pressure drop of component A (ΔP_A) from the catalyst surface to bulk gas stream is obtained from the following relations :

$$\Delta T = Q\,(j_H)^{-1}\,(P_r)_f^{2/3} \tag{5.3}$$

$$\Delta P_A/P_A = \Delta Y_a = R(j_d)^{-1}\,Y_{fA}\,(S_c)^{2/3} \tag{5.4}$$

where

$$Q = \frac{r_{MA}\,\Delta H_A}{a_M\,\varphi\,C_p\,G_M} \tag{5.5}$$

ΔH_A = molal heat of reaction of component A.

P_r = Prandtl number = $C_p\mu/k$.

R = $r_{MA} / a_M\,\varphi\,G_M$.

S_c = Schmidt number = $\mu / \rho D_{AM}$

Y_{fA} = P_{fA} / π

$$P_{fA} = \frac{(\pi + \delta_A P_A) - (\pi + \delta_A P_{Ai})}{\ln\left(\frac{\pi + \delta_A P_A}{\pi + \delta_A P_{Ai}}\right)} \tag{5.6}$$

$$\delta_A = \frac{r + s + \cdots\cdots a - b \cdots}{a}$$

where r , s , -----, a, b are coefficients in reaction equation ,

$$aA + bB + \cdots\cdots \rightarrow rR + sS + \cdots\cdots$$

π = total pressure.

D_{AM} = average diffusivity of component A.

G_M = molal mass velocity based on total cross section of bed.

G = mass velocity based on total cross section.

The values of j factors to be used are related with Reynold number $(G/a_v \varphi \mu)$

For $0.01 < R_e < 50$

$j_d = 0.84\ R_e^{-0.51}$

For

$50 < R_e < 1000$

$j_d = 0.57\ R_e^{-0.41}$

And

$j_H = 0.076\ j_d$

Where j_d and j_H are Chilton Colburn dimensionless j factors[48] Yoshida et al.[51] concluded that R_e and Q are the most important factors in controlling the pressure and temperature drops. Increasing the flow rate and decreasing the particle size reduces the resistance to heat and mass transfer.

A sample calculation based on the method of Yoshida is given in Appendix 8-E. From these calculations, it can be observed that the pressure and the temperature gradients were negligible.

2. Effect of process variables - The effect of temperature (T), weight of catalyst to methanol feed ratio (W/F) and the concentration of methanol in the feed (R) on conversion (X), yield of formaldehyde (Y), and selectivity (S) was studied. The experimental results are tabulated in Appendix 8-A.

For one particular value of W/F and R, the effect of temperature was studied in the range (300°C - 500°C). The results are plotted in figure 5.2. The effect of W/F at one particular temperature and $\bar{R}$ has been plotted in figures 5.3 to 5.11. The effect of concentration of methanol in feed can be observed in figures 5.12 to 5.14.

3. Correlation of data -

I. Initial Rate - The rate equation in a steady state flow system can be written as :

$$W/F = \int_{o}^{x} dx/r \qquad (5.7)$$

The initial rate is the rate of reaction at zero conversion. Yang and Hougen[45] have shown that by considering the effect of pressure on the initial rate, choice of mechanism can be reduced. Initial rate equations are obtained by neglecting partial pressure of products. The accuracy of this method is very limited as it is not possible to accurately find slopes at low conversion.

The initial rates were obtained by plotting conversion against W/F as shown in figures 5.12 to 5.14, and finding slope at W/F = 0. In figure 5.15 initial rates thus obtained have been plotted against methanol concentration in feed. Comparing these curves with those drawn by Yang and Hougen[45], it was concluded that the controlling step during the reaction was either adsorption of reactants or a surface reaction between the reactants.

II. Correlation of conversion data - Integrated rate equations as given in Table 3.1 can be rearranged in the form of $y = a_o + a_1 x$. The values of y, x, a_o and a_1 are listed in Table 5.1. y and x values were calculated for different values of W/F at one particular set of

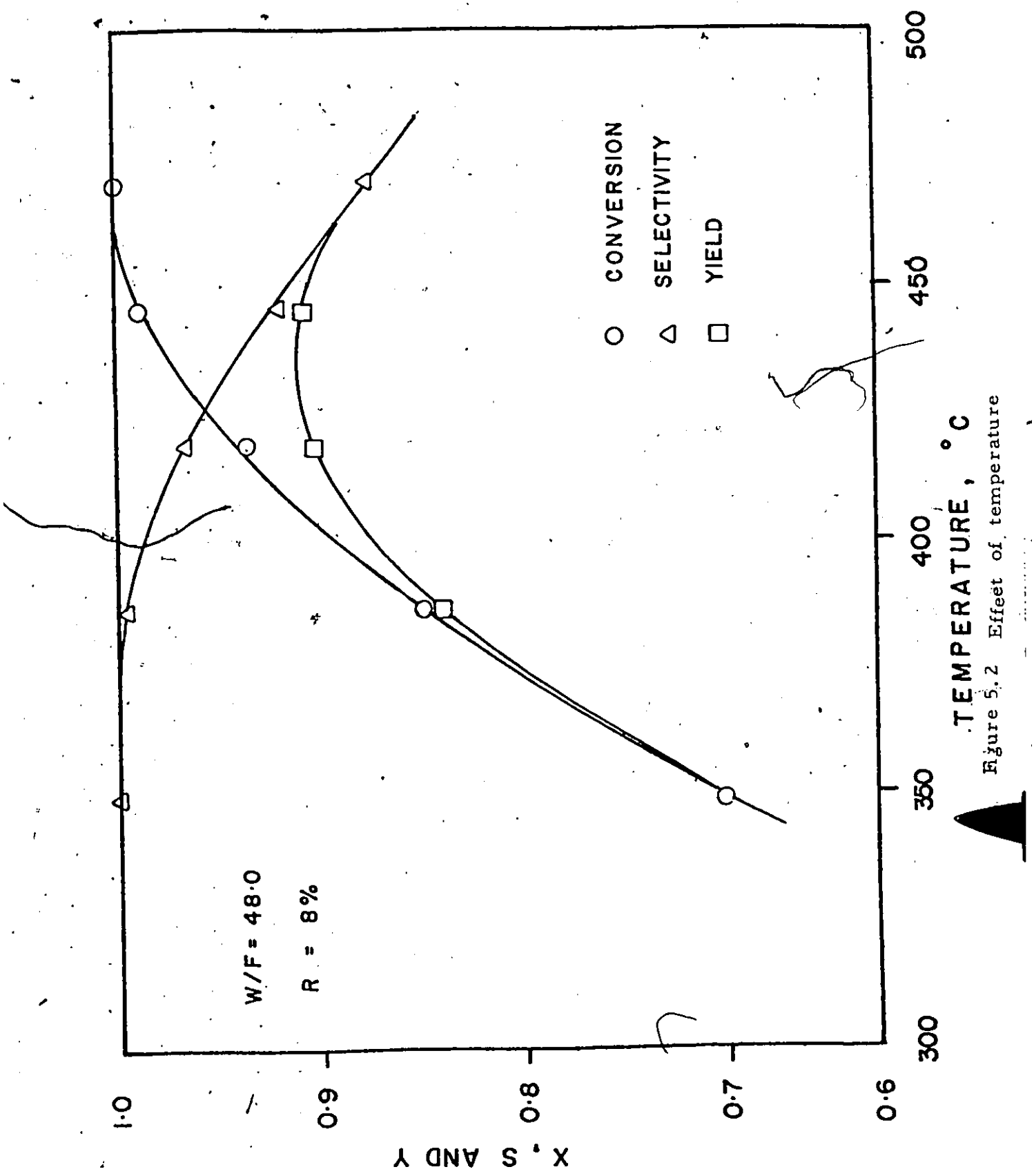

Figure 5.2 Effect of temperature

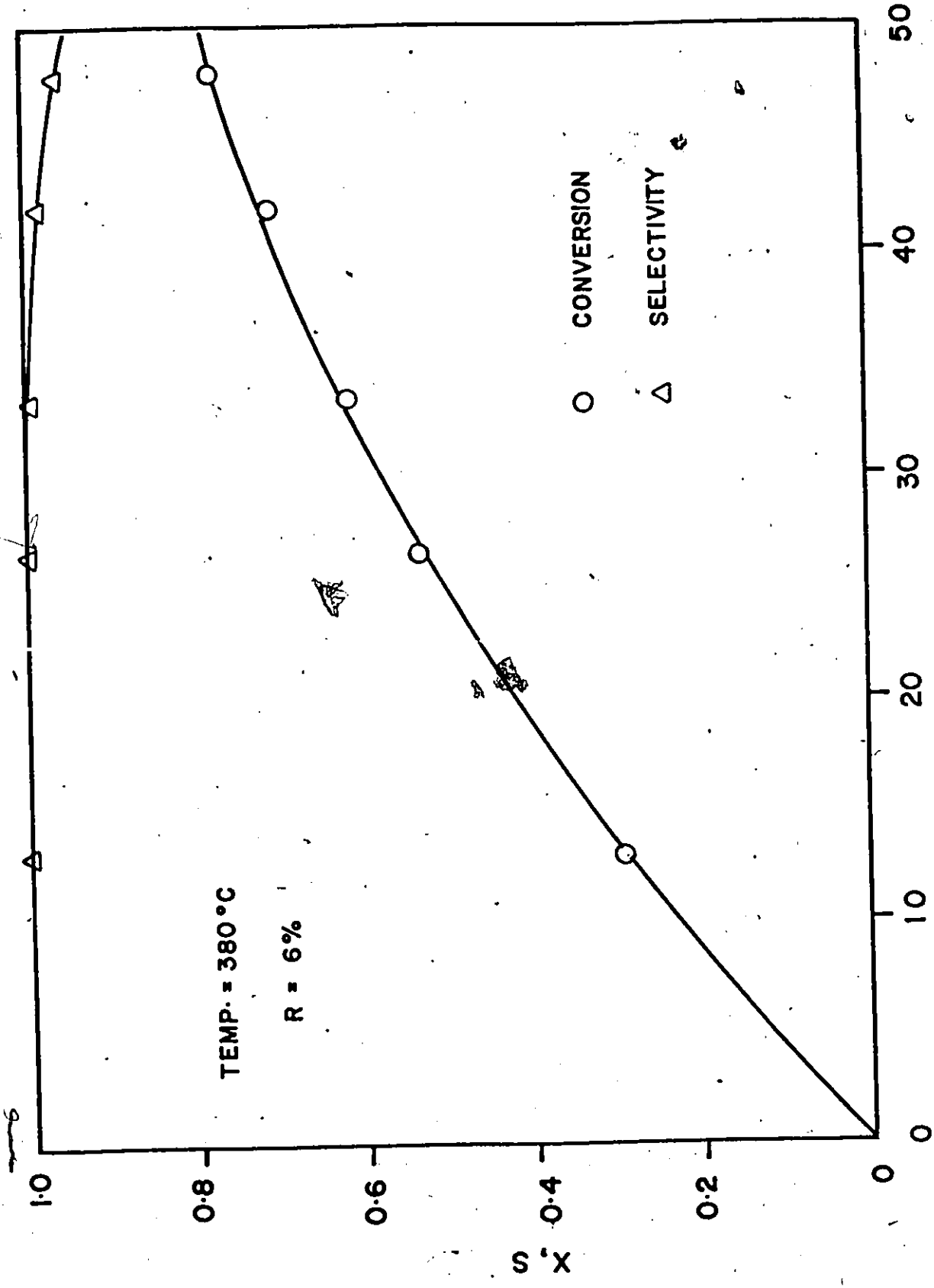

Figure 5.3 Effect of W/F (gm. hr /mole)

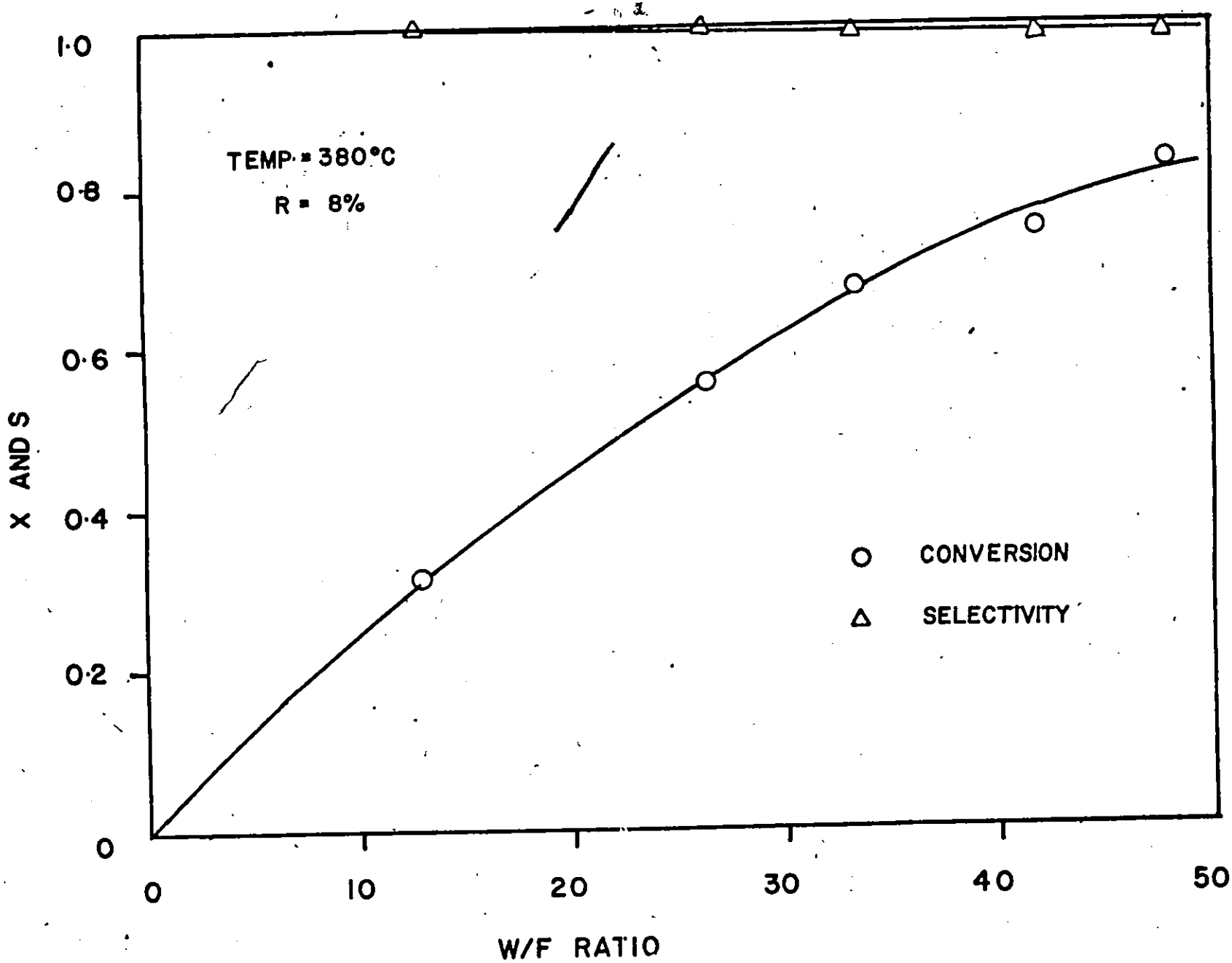

Figure 5.4 Effect of W/F (gm. hr./mole)

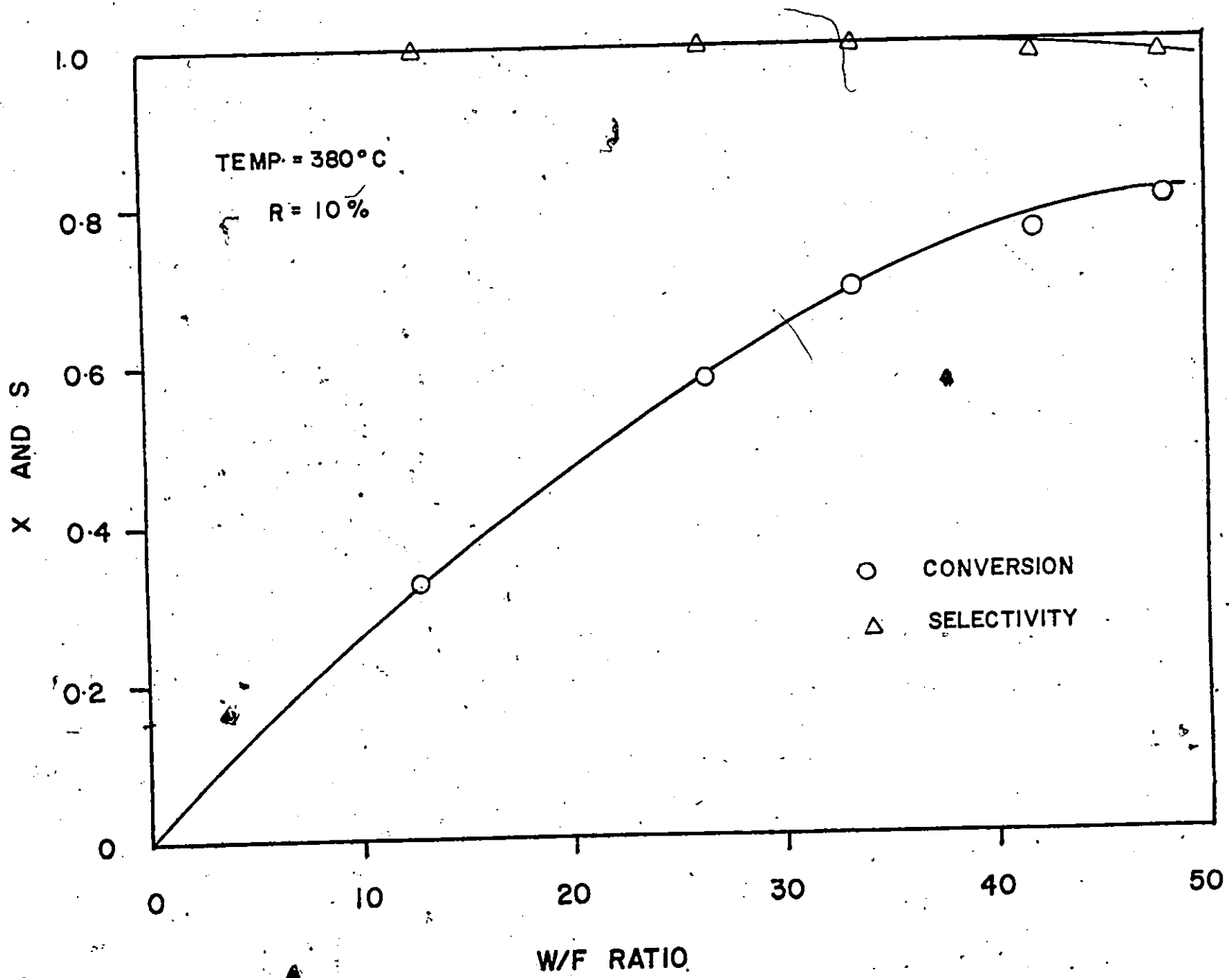

Figure 5.5 Effect of W/F(gm. hr. /mole) on conversion and selectvity

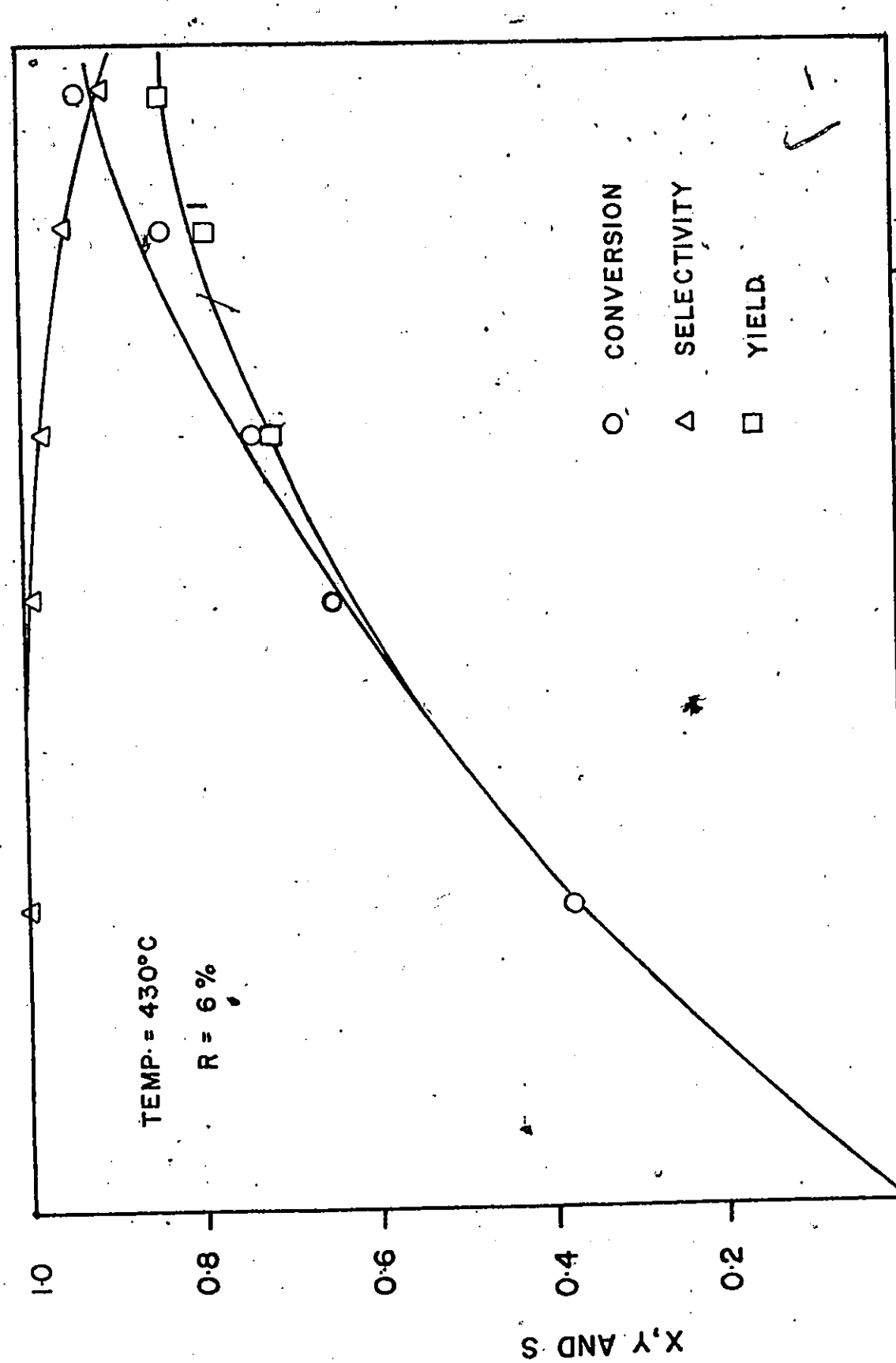

Fig. 5.6 Effect of W/F(gm. hr. /mole) on conversion, selectivity and yield

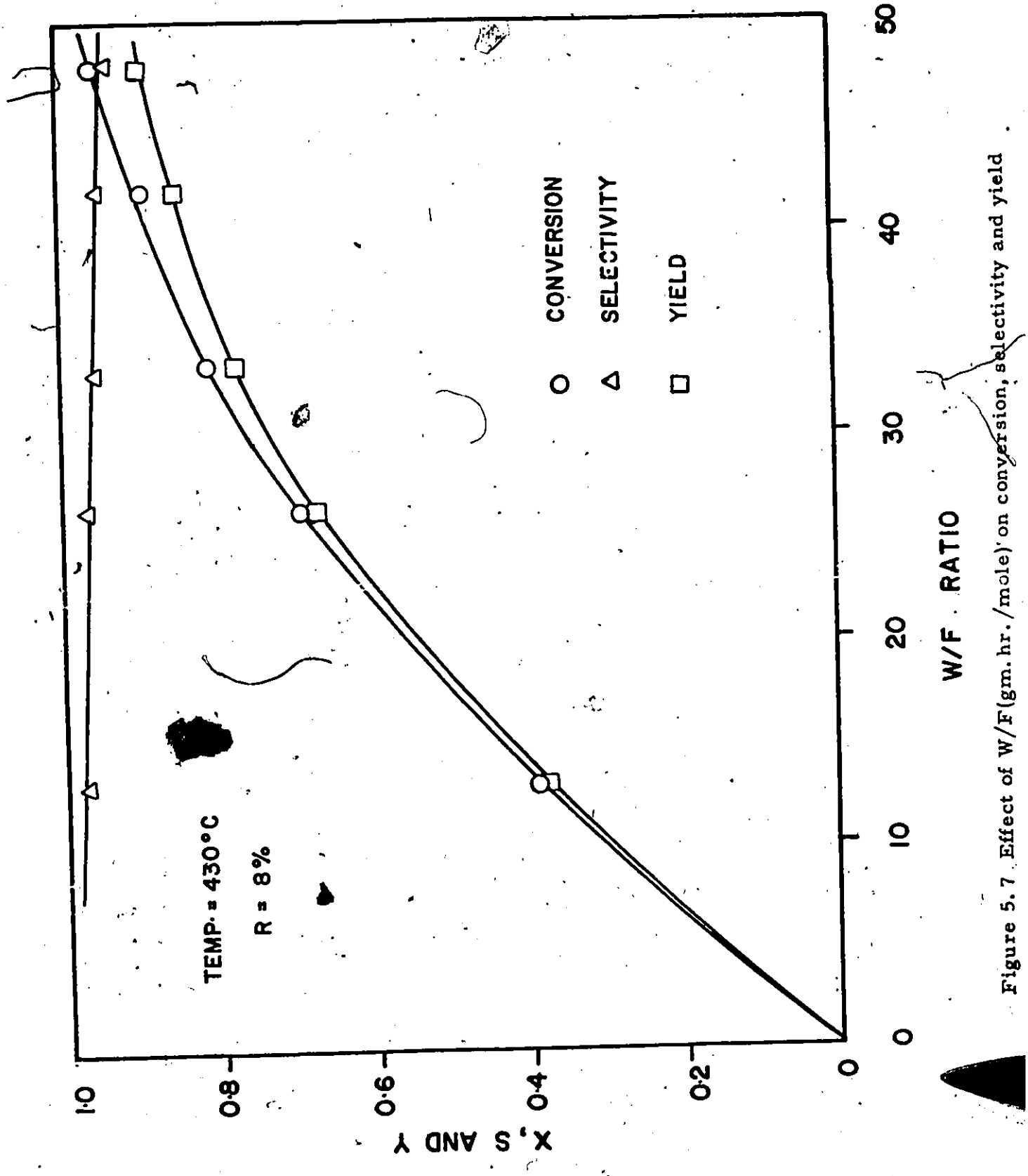

Figure 5.7 Effect of W/F(gm.hr./mole) on conversion, selectivity and yield

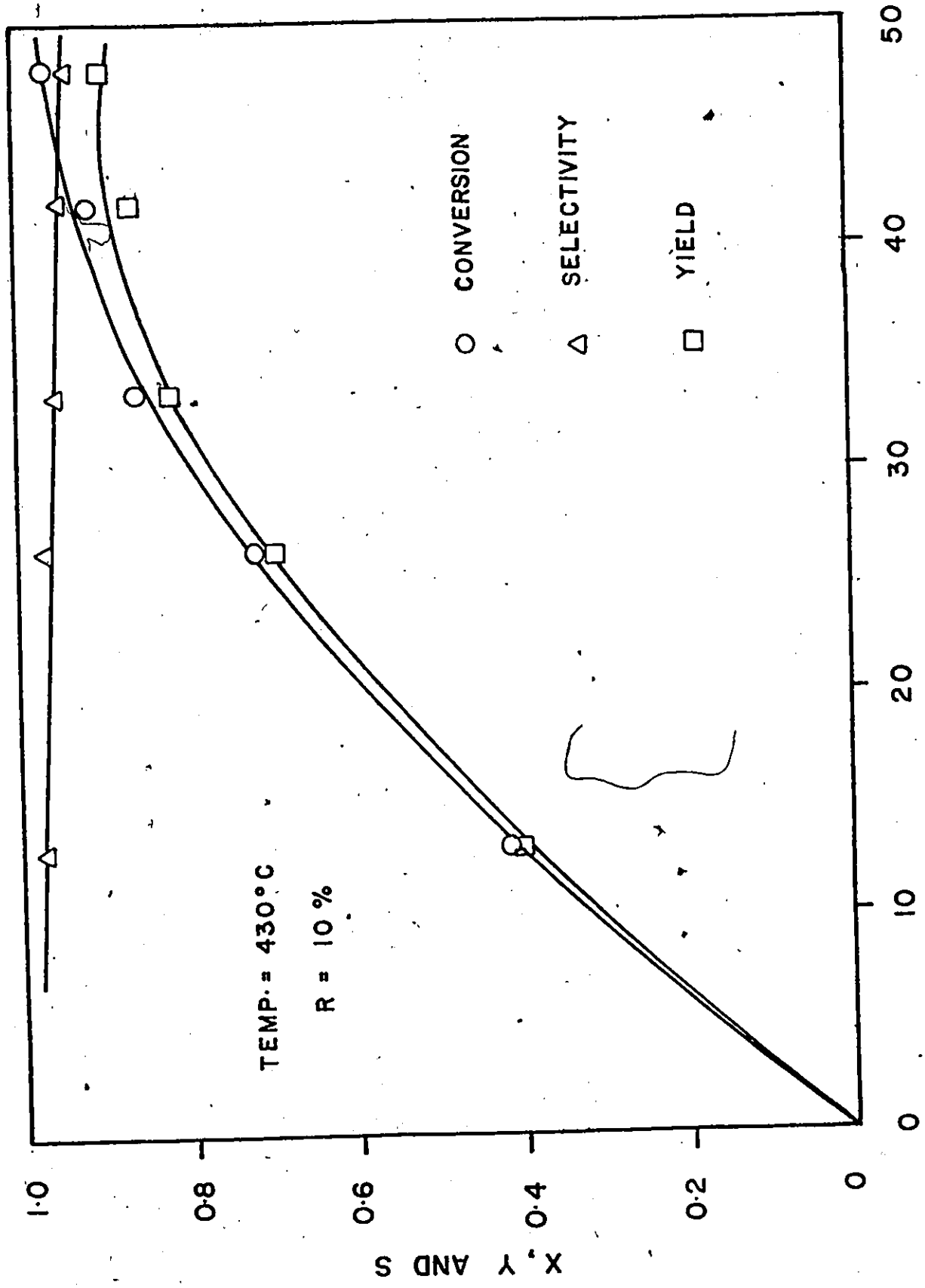

Figure 5.8 Effect of W/F(gm.hr./mole) on conversion, selectivity and yield

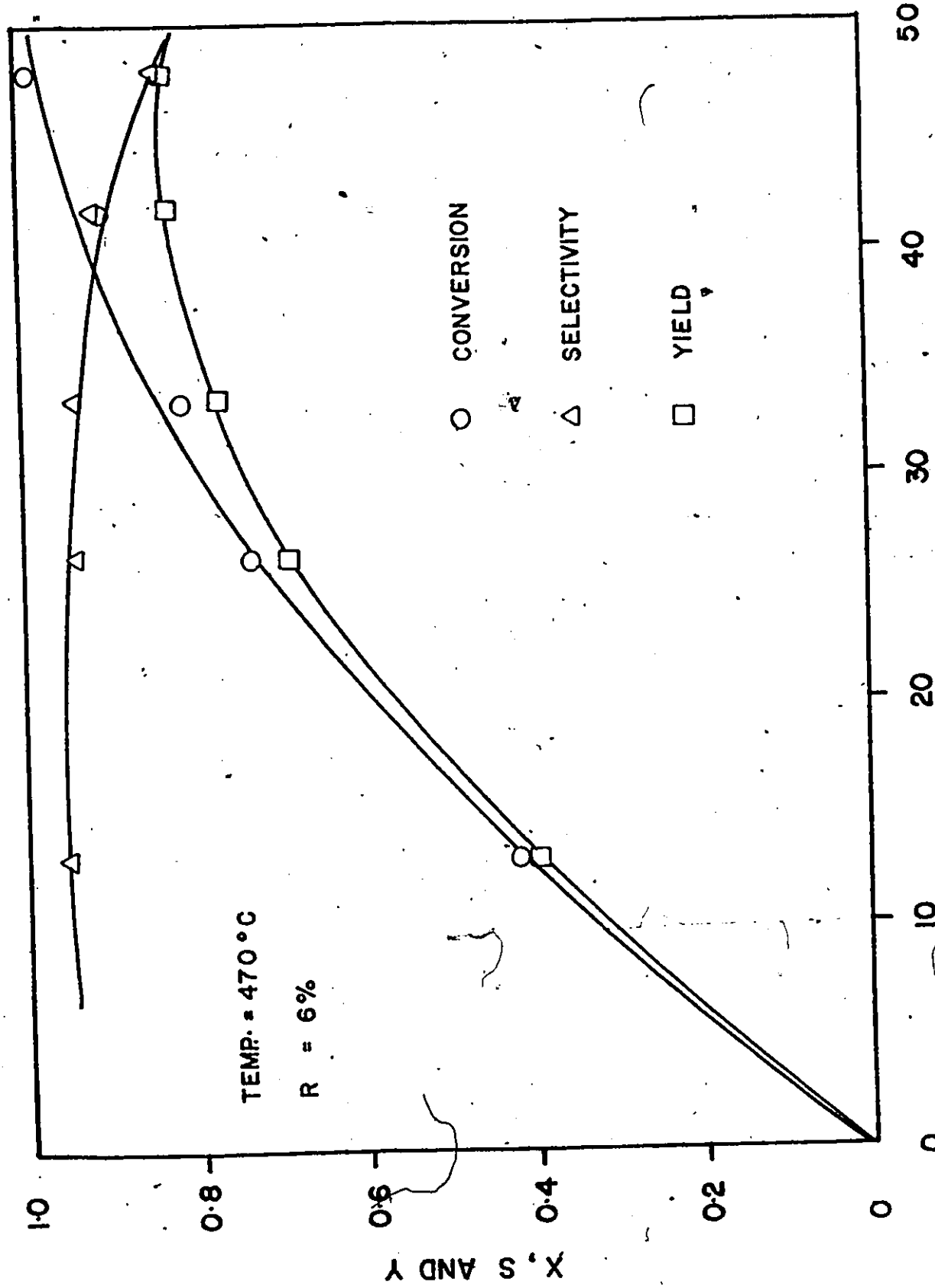

Figure 5.9 Effect of W/F(gm.hr./mole)

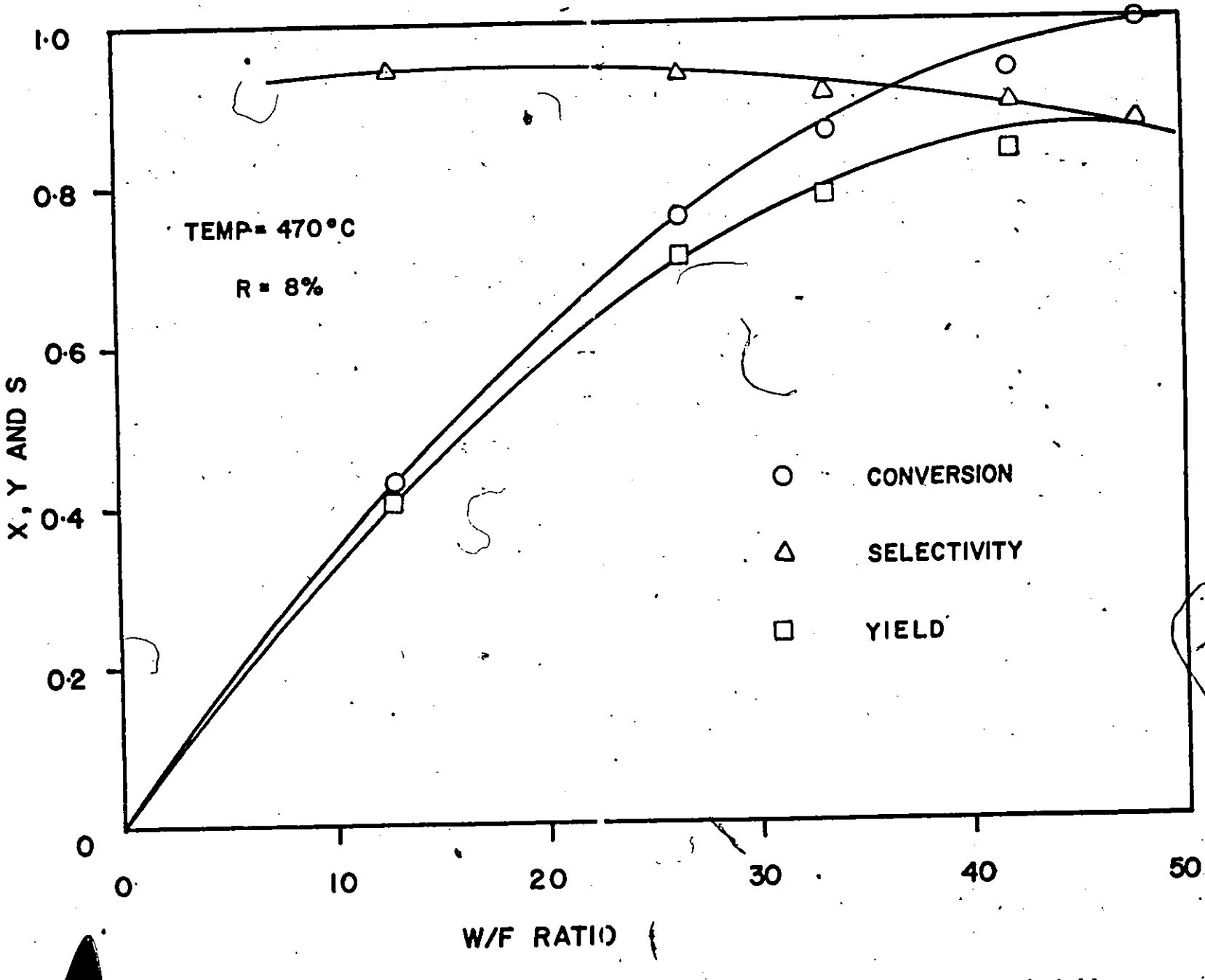

Figure 5.10 Effect of W/F(gm.hr./mole) on conversion, selectivityand yield

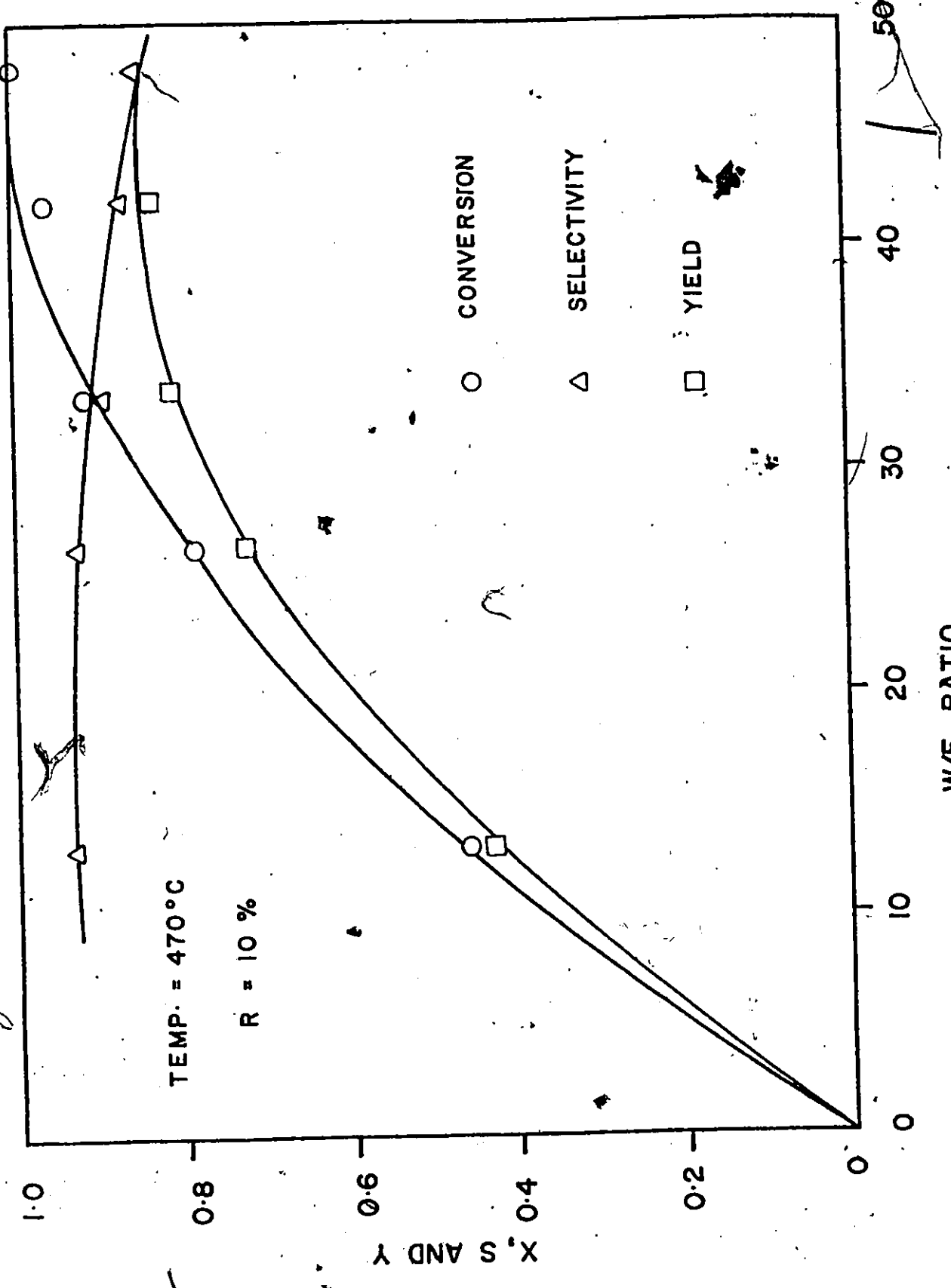

Figure 5.11 Effect of W/F (gm.hr./mole) on conversion, selectivity and yield

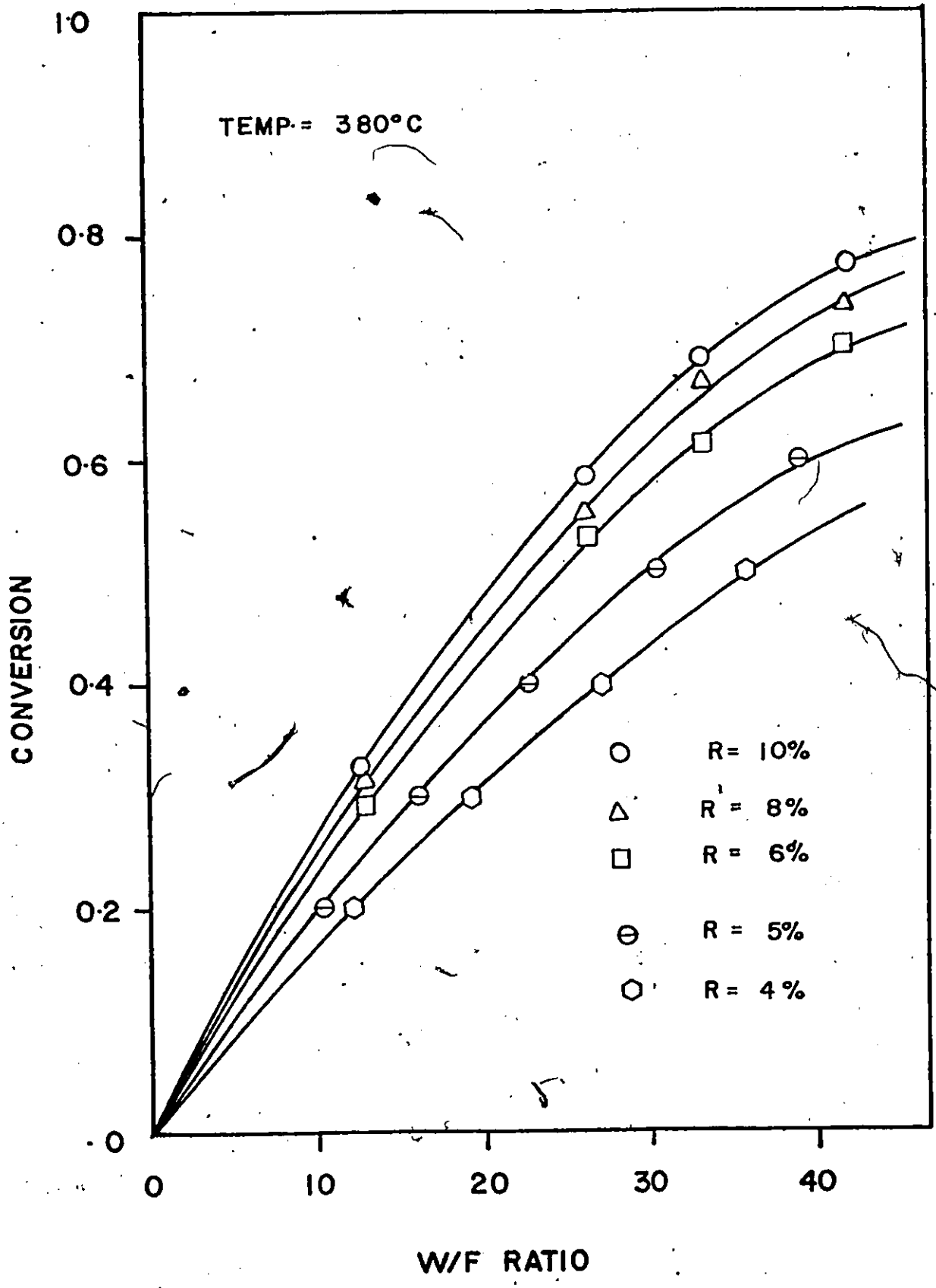

Figure 5.12 Effect of W/F (gm. hr./mole) on convrsion

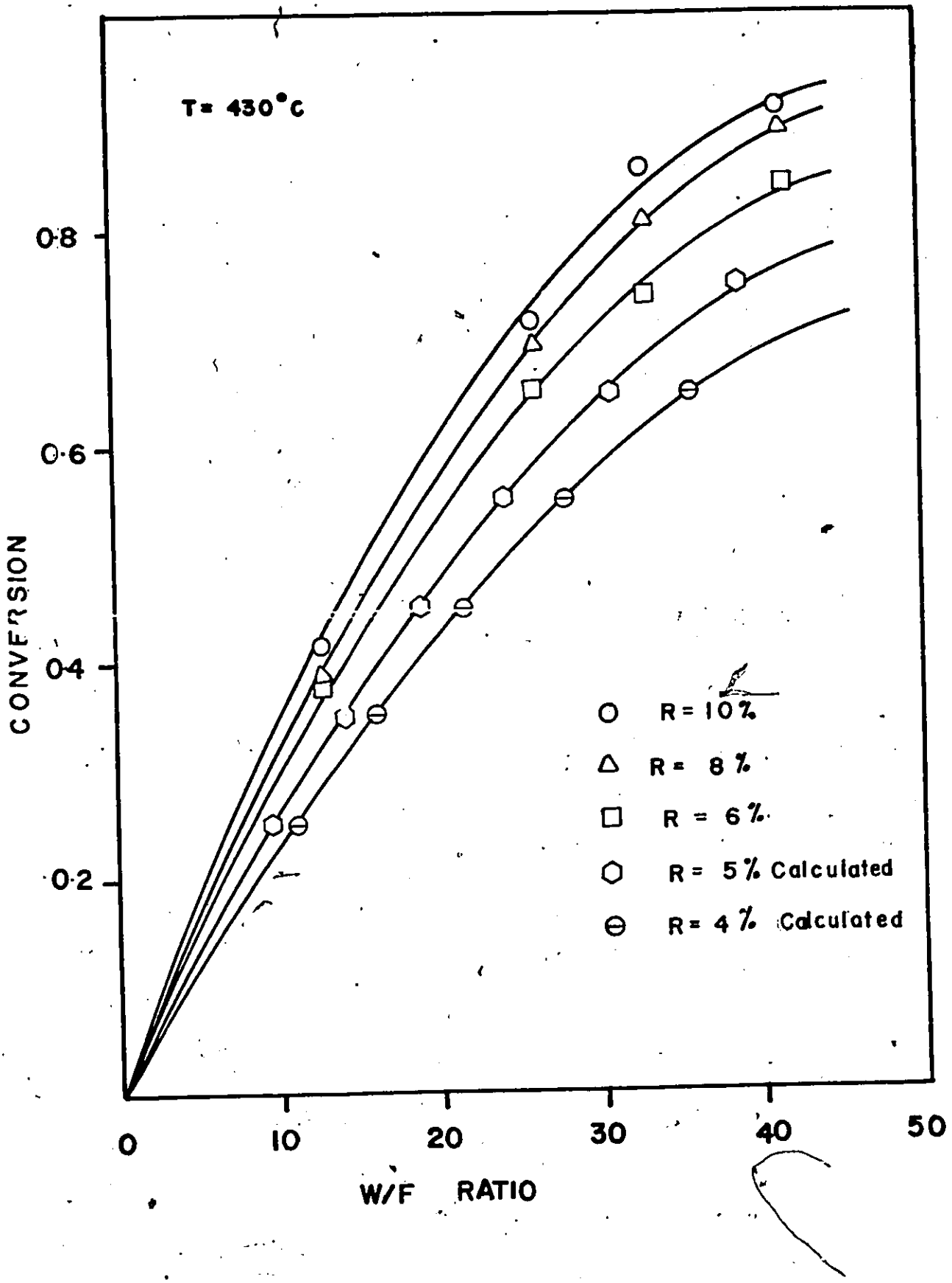

Figure 5.13 Effect of W/F(gm.hr./mole) on conversion

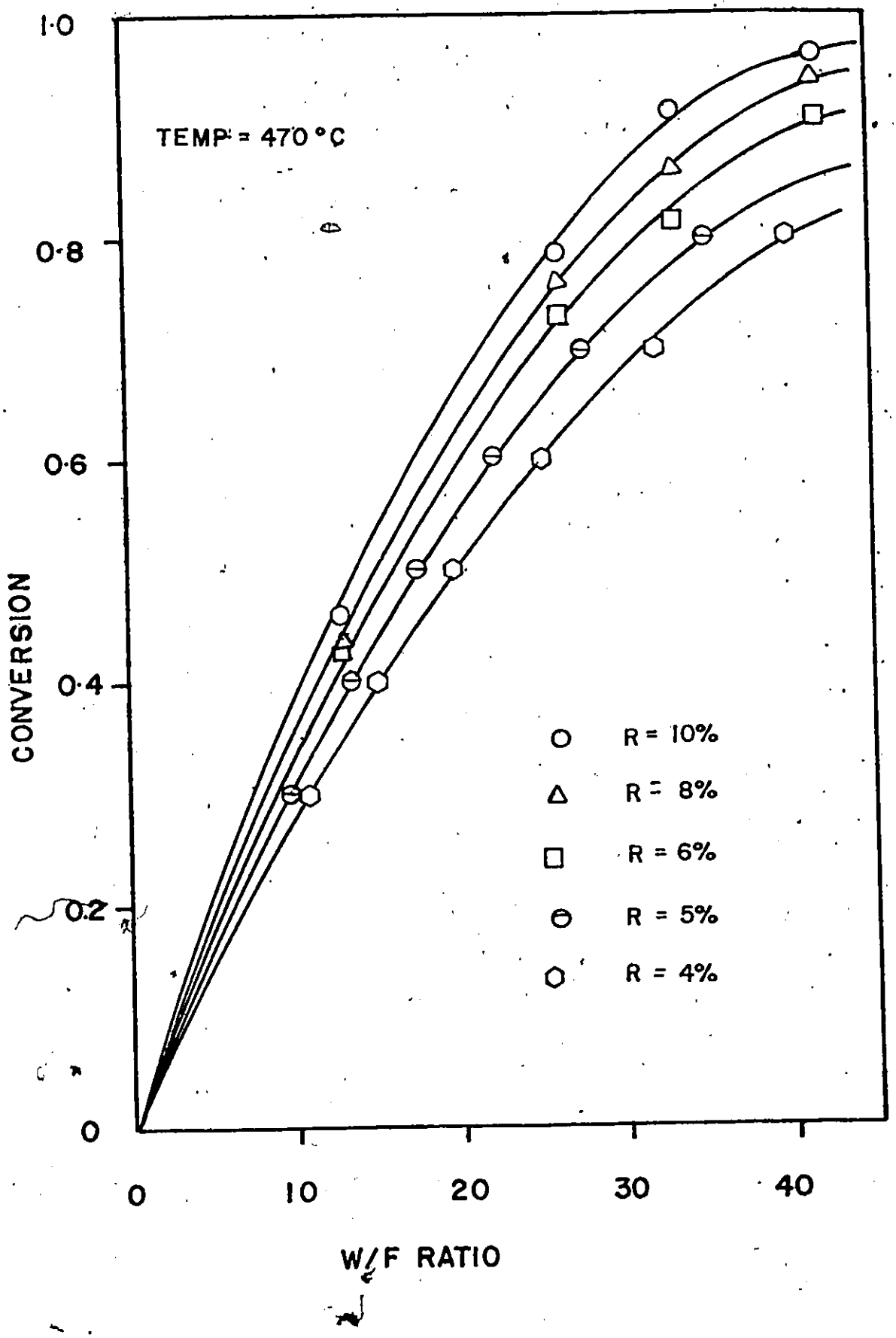

Figure 5.14 Effect of W/F(gm.hr./mole) on conversion

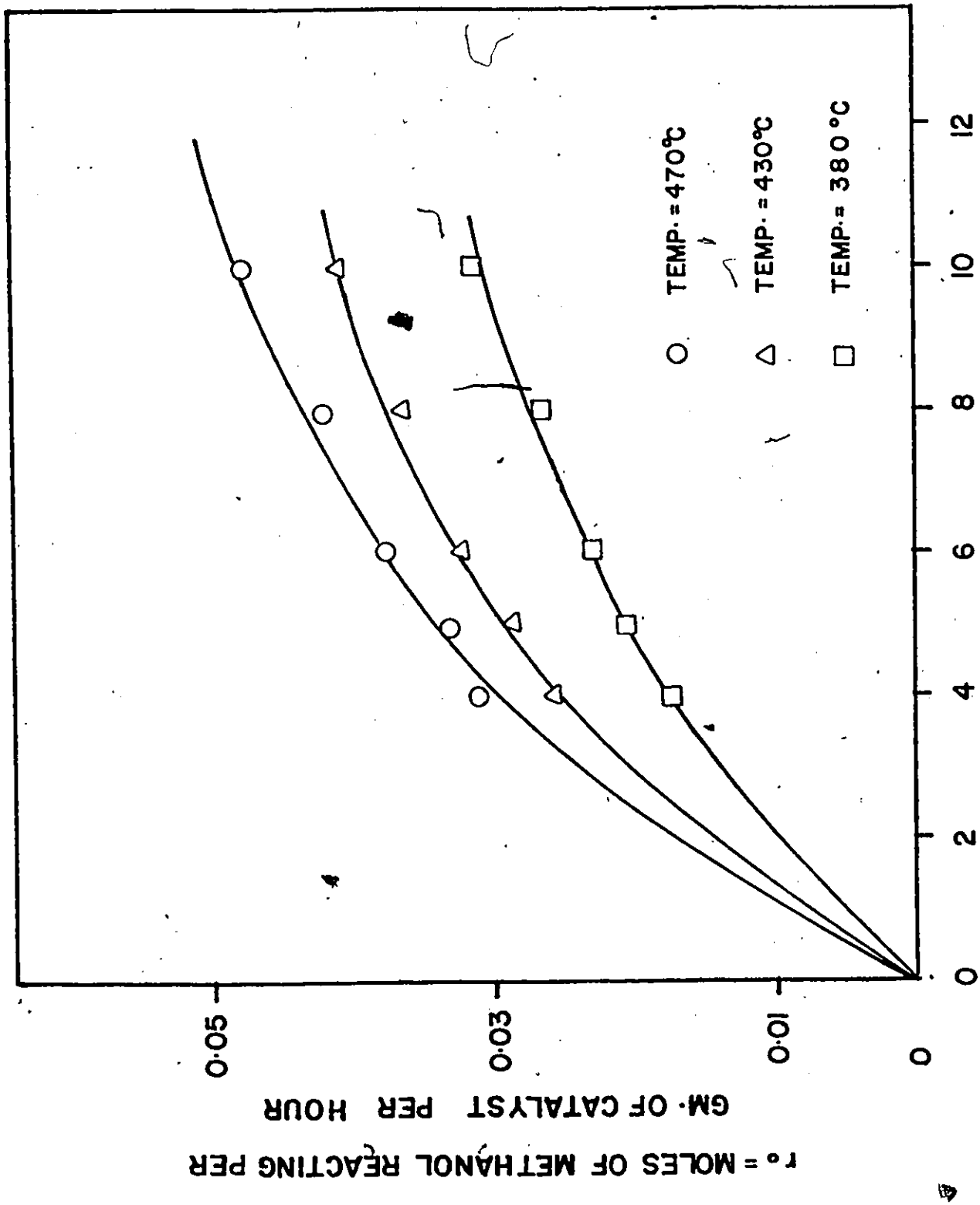

Figure 5.15 Initial rates vs mole% methanol in feed

Table 5-1

Correlated y and x Relations

No.	Reaction Order m (CH_3OH)	Reaction Order n (O_2)	a_o	a_1	y	x
1	1	0.5	$1/k_1$	$1/k_2$	$(-W/F)\left[{}_oP_M/\ln(1-x)\right]$	$\left[4\alpha/\ln(1-x)\right]$ $\left[({}_oP_{O_2} - x\,{}_oP_M/2)^{\frac{1}{2}} - {}_oP_{O_2}^{\frac{1}{2}}\right]$
2	1	0	$1/k_2$	$1/k_1$	$W/Fx\alpha$	$-\ln(1-x)/{}_oP_M x\alpha$
3	0.5	0	$1/k_2$	$1/k_1$	$W/Fx\alpha$	$2\left[1-(1-x)^{\frac{1}{2}}\right]/{}_oP_M^{\frac{1}{2}} x\alpha$
4	1	1	$1/k_1$	$1/k_2$	$-W\,{}_oP_M/F\ln(1-x)$	$\dfrac{-2\alpha\ln\left[{}_oP_{O_2}/({}_oP_{O_2} - \frac{1}{2}\,{}_oP_M x)\right]}{\ln(1-x)}$
5	0.5	0.5	$1/k_1$	$1/k_2$	$W\,{}_oP_M^{\frac{1}{2}}/2F\left[1-(1-x)^{\frac{1}{2}}\right]$	$2\alpha\left[{}_oP_{O_2}^{\frac{1}{2}} - ({}_oP_{O_2} - \frac{1}{2}\,{}_oP_M x)^{\frac{1}{2}}\right]$ $/{}_oP_M^{\frac{1}{2}}\left[1-(1-x)^{\frac{1}{2}}\right]$

conditions. A linear equation correlating y and x was obtained by plotting the data, and using the method of least square for drawing the straight line. Hence, for one particular temperature and R, K_1 and K_2 values were obtained. The rate equation with m=1 and n=0.5 was found to give the best possible fit. The rate expression can therefore be written as :

$$r = K_1 P_M / (1 + 0.5 K_1 P_M / K_2 P_{O_2}^{0.5}) \qquad (5.8)$$

Values of K_1 and K_2 for this particular mechanism are listed in Table 5.2. K_1 and K_2 values for other m and n, where experimental data did not fit are listed in Appendix 8-F. At different conversions obtained in the experimental data, W/F were calculated using values of K_1 and K_2. The values of W/F obtained experimentally are compared with values of W/F obtained theoretically in Appendix 8-D.

III. Temperature effect on rate constants - In Table 5.2 values of K_1 and K_2 at different temperatures are listed for m = 1 and n = 0. Log K_1 and Log K_2 were plotted against the inverse of temperature in °K as shown in figure 5.16 and 5.17. The reaction appears to follow Arrhenius law. The mathematical relations obtained from these plots are :

$$\text{Log } K_1 = -0.1637 - 1.930 \times 10^3/T \qquad (5.9)$$

$$\text{Log } K_2 = -2.515 - 312.87/T \qquad (5.10)$$

The slopes and intercepts of straight lines in figures 5.17 and 5.18 were obtained by plotting the data and drawing the straight line using the method of least square fit. The values thus obtained were used in the relations 5.9 and 5.10.

Table 5-2

Temperature Effect on Rate Constants

for m = 1 n=0.5

Temp. °C	R %	K_1 $\frac{\text{moles}}{\text{gm.-mm Hg-Hr}}$ $\times 10^3$	K_2 $\frac{\text{moles}}{\text{gm.-mm Hg}^{0.5}\text{-Hr}}$ $\times 10^3$
350	6.0	0.5794	1.0867
	8.0	0.7507	0.5730
	10.0	0.3887	1.0991
Overall value		0.5797	0.9196
380	6.0	0.7687	1.0357
	8.0	0.7397	1.0802
	10.0	0.5223	1.0617
Overall value		0.6769	1.0594
410	6.0	1.0716	1.2743
	8.0	1.0288	1.1083
	10.0	0.8733	1.2284
Overall value		1.0178	1.1772
430	6.0	1.5476	0.9776
	8.0	1.5533	0.9110
	10.0	1.2925	1.0134
Overall value		1.4645	0.9673
450	6.0	1.3387	1.3852
	8.0	1.5123	1.0483
	10.0	1.3616	1.1088
Overall value		1.4042	1.1808
470	6.0	1.6490	1.2310
	8.0	1.6683	1.0655
	10.0	1.6583	1.0672
Overall value		1.6586	1.1212

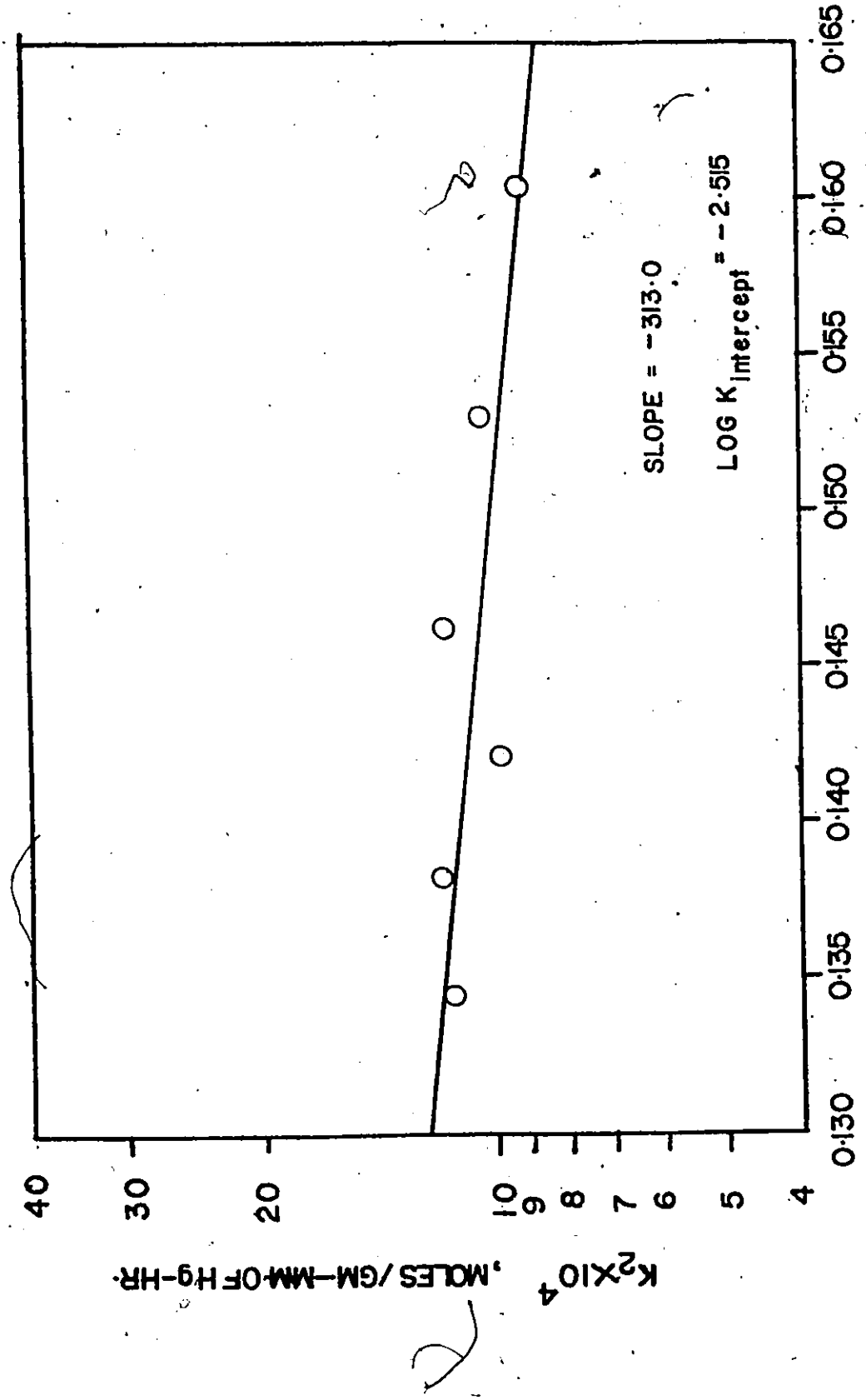

Figure 5.16 Temperature effect on Rate constant K_2

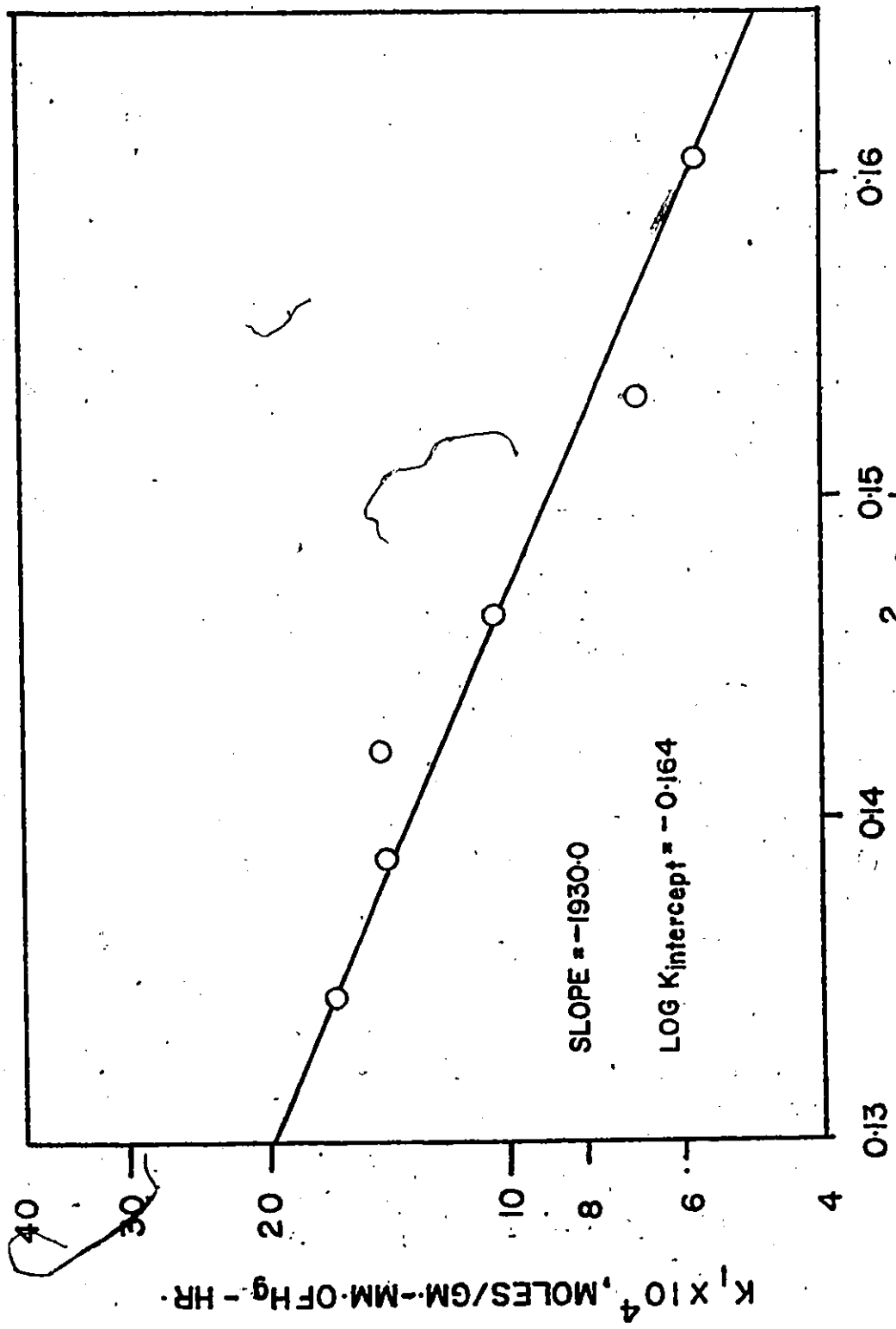

Figure 5.17 Temperature effect on Rate constant K_1

The activation energy of the two steps of the reaction calculated from the equations 5.9 and 5.10 were equal to 8.8 K cals/mole and 1.4 K cals/mole respectively.

VI. DISCUSSION

The kinetics of methanol oxidation has been investigated in the temperature range 300 - 500°C over tungsten trioxide-molybdenum-trioxide mixture as catalyst, and a possible rate mechanism has been proposed. Arnold[36], Popov[34] and Liminov et al.[41] have studied the effect of various process variables and the catalyst composition for methanol oxidation over molybdenum-tungsten oxide catalyst. However, no detailed work has been carried out to propose a kinetic rate expression for methanol oxidation over MoO_3-WO_3 catalyst.

Pure molybdenum trioxide has been found to be highly selective to formaldehyde formation. This has been very well established by a number of workers[12, 52, 2, 3]. The use of pure molybdenum trioxide, however, results in low overall conversion of methanol, generally less than 50%. A number of other metal oxide catalysts such as vanadium penta-oxide[2, 52], manganese oxide[3] and iron oxide[3] have been studied for the oxidation of methanol. These oxides have been found to be very active for the reaction. However, selectivity for the formaldehyde formation remains low. In order to obtain higher conversion of methanol without sacrificing the selectivity, a number of attempts have been made to use composite catalysts made of molybdenum trioxide and more active transition metal oxides. Tungsten trioxide-molybdenum trioxide is one such combination on which not enough studies have been carried out so far, even though tungsten trioxide has been proved to be an active catalyst for methanol oxidation[41]. Further, it may not have been uncommon

to anticipate, that tungsten and molybdenum being in the same group of the periodic table, catalytic performance of their oxides should remain similar. However, experimental data on tungsten trioxide has shown it to be a very active catalyst for this particular reaction. Hence, an attempt has been made to study the kinetics of methanol oxidation over composite catalyst of molybdenum and tungsten oxides in the present investigation.

A preliminary study of the effect of the composition of the catalyst showed (Figure 5.1) that the conversion of methanol increased significantly as tungsten trioxide content in the catalyst mixture was increased. This behaviour was expected, because tungsten trioxide has been established to be more active than molybdenum trioxide by several workers (Chapter 2). The selectivity remained 100% till the tungsten trioxide content in the catalyst was up to 20%, beyond which selectivity showed a decline. The effect of the catalyst composition was studied, keeping all other process variables constant. The maximum yield of formaldehyde under these conditions was obtained when tungsten trioxide content in the catalyst was 45%. The other data available in the literature[41] suggested that maximum yield of formaldehyde is obtained for the catalyst mixture containing within 44% - 54% tungsten trioxide. Hence, a mixed catalyst composed of 45% WO_3 - 55% MoO_3 was selected for a detailed kinetic study of methanol oxidation reaction.

The effect of different operating variables has been described in Chapter V. An increase in the temperature resulted in an increase in the overall conversion of methanol. However, the selectivity to formaldehyde formation generally decreased due to further oxidation to carbon oxides beyond 400°C. The partial pressure of the reactants was varied by changing the air flow rate through catalyst bed, while keeping the methanol feed rate constant. It was observed that the increase in the partial pressure of methanol resulted in the corresponding increase in the conversion of methanol. The change in the selectivity was negligible

when partial pressure of methanol was changed. Figures 5.2 - 5.11 show the effect of the W/F ratio on conversion, selectivity and the yield. The increase in the W/F ratio caused an increase in the conversion without affecting the selectivity significantly. Similar results have been reported in the literature for other metal oxide catalysts.

The Hougen Watson method based on the Langmuir-Hinshelwood mechanism, and the initial rate technique were used for the kinetic analysis of data. The value of the equilibrium constant K_p for methanol oxidation are of the order of 10^{12} at 250 °C and 10^{18} at 450 °C, while the values of free energy change (ΔG) for the reaction varies from -22.7 Kcals/mole at 527 °C to -26.2 Kcals/mole at 25 °C. Hence, this reaction could be considered highly irreversible.

The mechanism and the general kinetics of the reaction over tungsten-molybdenum oxide has been found to be similar to that obtained by Jiru et al.[24], Mars et al.[26], Bhaltacharya et al.[52] and Dosi[2] over other metal oxide catalysts.

Jiru[24] studied the kinetics of methanol oxidation over iron-molybdenum oxide catalysts at 270 °C. The two stage oxidation reduction mechanism was confirmed by determining the rate of interaction between methyl alcohol and the catalyst without the participation of oxygen in the gaseous phase and the rate of interaction between oxygen and partially reduced catalyst without the participation of methyl alcohol in the gaseous phase. Mars and Krevelin[26] studied the oxidation of aromatic hydrocarbons on vanadium pentaoxide catalyst. The results of Jiru, Mars and Bhaltacharya[52] suggested that the lattice oxygen ions in the catalyst particles interacted with methanol during the oxidation reaction.

Shelstad[53, 54] and Ioffe[55] also suggested 'two stage' redox mechanism for the oxidation of methanol over metal oxide catalysts, but argued against lattice oxygen taking part in the reaction. They favoured the mechanism by which the oxygen adsorbed on the catalyst surface reacted with methanol.

It is reasonable to assume as a starting point that the reaction takes place on the catalyst surface by one of the following two mechanisms : -

(1) Methanol reacts with lattice oxygen of catalyst giving a reduced catalyst. The reduced catalyst then reacts with molecular oxygen in the gaseous phase.

(2) Adsorbed oxygen on the catalyst surface reacts with methanol in the gaseous phase and the rate of removal of adsorbed oxygen from the catalyst surface is equal to the rate of adsorption of oxygen on the catalyst surface.

It is difficult to prove the participation of lattice oxygen in the catalytic oxidation process in the manner described by Jiru. Though it is possible that lattice oxygen does particpate in the reaction, in Jiru's experiments, as described earlier, oxygen could have been adsorbed by the oxide catalyst, and when methanol was injected into the reactor in the absence of air, it reacted with adsorbed oxygen. Gresmundo[37] carried out ESR studies on iron and vanadium oxide catalysts and established that lattice oxygen does participate in the reaction. It is also possible that reaction takes place by both of the above mentioned mechanisms and lattice oxygen participates in the reaction when adsorbed oxygen is lacking. The change in the colour of the catalyst, as observed by Jiru, indicated possible change in the structure of the catalyst. However, for tungsten trioxide-molybdenum trioxide catalyst, no ESR studies or other relevant studies have been reported in the literature, which might be helpful in drawing any definite conclusion regarding the choice between the above two mechanisms.

During present investigations, a change in the colour of the catalyst was observed when methanol was passed through the catalyst bed in the absence of air. The catalyst returned to the original colour in the presence of oxygen. It is therefore possible that methanol reacted with lattice oxygen of the catalyst. Both the mechanisms as discussed above,

the first in which lattice oxygen atoms react with the reactants, and the second in which the adsorbed oxygen molecules or atoms (not lattice oxygen) are removed from catalyst surface, however lead ultimately to the same rate expression. The two stage oxidation reduction mechanism would not be applicable in the case where the catalyst is participating in some other ways, involving three or more oxidation reduction stages.

As an initial step, it was attempted to fit the experimental data in the rate expressions derived on the basis of the 'two stage' redox mechanism for different values of reaction order m and n. The experimental data fitted very well in the rate expression derived on the basis of the 'two stage' mechanism with $m = 1.0$ and $n = 0.5$.

The rate constants for two steps, K_1 and K_2 fitted reasonably well in a straight line when log K_1 and log K_2 were plotted against inverse of temperature in °K (Figures 5.16 and 5.17). This shows that in the temperature range 300 - 500°C, two steps of reaction followed Arrhenius equation.

The initial rate plots when compared with the initial rate curves of Yang and Hougen suggested that either adsorption of reactants on the surface of catalyst or surface reaction or both controlled the reaction. This again confirmed that either one or both the steps in the rate mechanism proposed, controlled the reaction. Activation energy for the two steps calculated were 8.8 Kcals/mole for methanol reacting on the surface of the catalyst, and 1.4 Kcals/mole for the reduced catalyst reacting with oxygen in gaseous phase. It can be concluded from these values that the first step in the reaction offers much higher resistance for methanol oxidation compared to second step. Activation energies for V_2O_5 - MoO_3 catalyst[2] have been found to be 10.8 Kcals/mole and 9.3 Kcals/mole respectively for the two steps.

A significant difference between tungsten trioxide-molybdenum trioxide catalyst and iron-molybdenum oxide catalyst or vanadium-

molybdenum oxide catalyst is that no new compound is formed in the first case. It has been established by a number of workers (Chapter 2) that iron molybdate and vanadium molybdate are active components for these catalysts. Liminov[41] found by x-ray studies that no new compound is formed for tungsten-molybdenum oxide catalysts and also observed that $WO_3 \cdot MoO_3$ are active sites for methanol oxidation reaction.

Further studies have to be carried out with the reduced catalyst in order to find as to how catalyst surface participates in the reaction. The change in the colour of the catalyst, indicated that probably lattice oxygen is being removed from catalyst particles. It has been proved from the present investigations that reaction takes place in 'two steps' by oxidation reduction mechanism for tungsten trioxide-molybdenum trioxide catalyst. It has also been observed that activation energies for the two steps of methanol oxidation reaction over WO_3-MoO_3 catalyst are lower compared to those obtained on other metal oxide catalysts.

The tungsten trioxide-molybdenum trioxide catalyst gave very high yield of formaldehyde and proved to be a promising catalyst for industrial use. The present work also provides a background for further studies on the WO_3-MoO_3 catalyst as regards its surface and the structure.

VII . CONCLUSIONS

On the basis of initial runs taken for different catalyst compositions, a catalyst containig 45% Tungsten trioxide and 55% Molybdenum trioxide was selected for the detailed kinetic study of oxidation of methanol to formaldehyde.

Experiments were carried out for W/F ratios between 13.0 to 48.0 gm. hr./gm. mole . Feed contained from 6 to 10 mole% methanol. Temperature was changed from 300°C to 500°C.

This catalyst proved to be highly active and selctive to formaldehyde formation. Conversion upto 100% and yield of formaldehyde upto 90.7% were obtained. Maximum yield was obtained at W/F ratio =48.0 for a methanol concenteration in feed of 10% and a temperature of 426°C. The conversion at these operating conditions was 95.6%.

Rate equation for the oxidation of methanol to formaldehyde was derived on the basis of a two stage redox mechanism. According to this mechanism -

$$CH_3OH(g) + s_{ox.} \xrightarrow{K_1} HCHO(g) + H_2O(g) + s_{red.} \qquad (7.1)$$

$$O_2(g) + s_{red.} \xrightarrow{K_2} s_{ox.} \qquad (7.2)$$

Where $s_{ox.}$ represents an active site of lattice or adsorbed oxygen. $s_{red.}$ represents reduced site of lattice oxygen or the empty site.

The rate equation for the temperature range of 300°C to 470°C which correlated the data most satisfactorily was-

$$r = \frac{K_1 \cdot p_M}{1 + K_1 \cdot p_M / 2 K_2 \cdot p_{O_2}^{0.5}} \qquad (7.3)$$

Where K_1 and K_2 are the temperature dependent rate constants of steps one and two. The equations relating K_1 and K_2 with temperature were-

$$\text{Log } K_1 = -0.1637 - 1.930 \times 10^3 / T \qquad (7.4)$$

$$\text{Log } K_2 = -2.5151 - 312.87 / T \qquad (7.5)$$

The activation energies of two steps , evaluated by comparing equations 7.4 and 7.5 with the Arrhenius equation were 8.8 K cals/mole and 1.4 K cals/mole.

VIII. APPENDIX

(A) EXPERIMENTAL DATA

Table 8-A-1 shows the effect of catalyst composition on conversion, selectivity and yield. The different conditions used for these runs were

Methanol feed rate $= 21.0 \times 10^{-6}$ moles/sec.

W/F Ratio = 32.0

%of Methanol in feed= 8%

Temperature = 440°C

Tables 8-A-2 to 8-A-16 show the effect of various process variables on conversion, selectivity and yield. Methanol flowrate in all runs was 21.0×10^{-6} moles/sec. . Catalyst used for these runs contained 45% Tungsten trioxide and 55% Molybdenum trioxide.

Table 8-A-1

W/F=32.0, R=8%, Temp.=440°C

Run No.	Catalyst comp. %MoO_3	O_2/N_2	CO_2/N_2	CO/N_2	F_{O_2} mol /sec. x10^6	F_{CO_2} mol./sec. x10^6	F_{CO} mol./sec. x10^6	W/T
1	100	0.2477	0	0	47.045	0	0	0.3102
2	70	0.2265	0	0	43.010	0	0	0.4446
3	50	0.2019	0.006	0.0056	38.342	1.1415	1.0763	0.5218
4	30	0.1911	0.0126	0.0197	36.292	2.3940	3.7359	0.6374
5	0	0.1824	0.0129	0.0380	34.645	2.4450	7.2120	0.7421

Run No.	F/T_1	M/T mol/sec. x10^6	F_f mol./sec x10^6	F_m mol/sec x10^6	T mol/sec x10^6	Con. X%	Select. S%	Yield Y%
1	0.2849	0.4049	8.3682	11.890	29.3689	41.30	100.0	41.30
2	0.3992	0.1563	13.9528	5.4604	34.9535	71.87	100.0	71.87
3	0.4083	0.0693	16.0572	2.7216	39.2757	87.04	87.86	76.47
4	0.3387	0.0239	13.8947	0.9795	41.0500	95.34	69.3	66.07
5	0.2579	0	10.6546	0	41.3130	100.0	52.40	52.40

Table 8-A- 2

W/F = 13.0, R = 6%

Run No.	Temp. °C	O_2/N_2	CO_2/N_2	CO/N_2	F_{O_2} mol./sec. x10^6	F_{CO_2} mol./sec. x10^6	F_{CO} mol./sec. x10^6	W/T
6	338	0.2573	0	0	66.870	0	0	0.1850
7	384	0.2535	0	0	65.898	0	0	0.2540
8	412	0.2519	0.0004	0.0005	65.483	0.0982	0.1388	0.2996
9	452	0.2500	0.0012	0.0009	64.991	0.2982	0.2249	0.3370

Run No.	F/T	M/T	F_f mol$_6$/sec. x10^6	F_m mol$_6$/sec. x10^6	T mol$_6$/sec. x10^6	Con. X%	Selct. S%	Yield Y%
6	0.1549	0.6601	3.8480	16.4035	24.8487	19.0	100.0	19.0
7	0.2261	0.5199	6.1361	14.1074	27.1368	30.3	100.0	30.3
8	0.2416	0.4587	6.7672	12.8463	28.0049	35.29	96.6	34.09
9	0.2532	0.4098	7.2978	11.8123	28.8215	39.8	93.4	37.17

Table 8-A-3

W/F = 13.0 , R = 8%

Run No.	Temp. °C.	O_2/N_2	CO_2/N_2	CO/N_2	F_{O_2} mol./sec. $\times 10^6$	F_{CO_2} mol./sec. $\times 10^6$	F_{CO} mol./sec. $\times 10^6$	W/T.
10	340	0.2574	0	0	48.880	0	0	0.1815
11	384	0.2524	0	0	47.948	0	0	0.2586
12	414	0.2386	0	0.0011	45.304	0	0.2095	0.3081
13	456	0.2356	0.0004	0.0017	44.743	0.0748	0.3173	0.3452

Run No.	F/T	M/T	F_f mol./sec. $\times 10^6$	F_m mol./sec. $\times 10^6$	T mol./sec. $\times 10^6$	Con. X%	Selct. S%	Yield Y%
10	0.1656	0.6529	4.1669	16.4320	25.1676	20.2	100.0	20.2
11	0.2404	0.5009	6.6481	13.8495	27.6489	32.4	100.0	32.4
12	0.2511	0.4407	7.1127	12.4833	28.3229	36.9	97.2	35.9
13	0.2637	0.3911	7.6630	11.3627	29.0060	41.5	95.1	39.46

Table 8-A-4

W/F = 13.0, R = 10%

Run No.	Temp. °C	O_2/N_2	CO_2/N_2	CO/N_2	F_{O_2} mol./sec. x10^6	F_{CO_2} mol./sec. x10^6	F_{CO} mol./sec. x10^6	W/T
14	340	0.2572	0	0	38.400	0	0	0.1929
15	385	0.2502	0	0	37.358	0	0	0.2588
16	416	0.2398	0.0004	0.0011	35.797	0.0599	0.1697	0.3143
17	463	0.2295	0.0010	0.0026	34.264	0.1455	0.3943	0.3613

Run No.	F/T	M/T	F_f mol$_6$/sec. x10^6	F_m mol$_6$/sec. x10^6	T mol$_6$/sec. x10^6	Con. X%	Selct. S%	Yield Y%
14	0.1691	0.6381	4.2728	16.1262	25.2736	20.9	100.0	20.9
15	0.2480	0.4933	6.9240	13.7745	27.9246	33.45	100.0	33.45
16	0.2651	0.4206	7.6587	12.1504	28.8890	39.36	97.10	38.22
17	0.2762	0.3422	8.2196	10.6943	29.7601	45.02	93.80	42.25

Table 8-A-5

W/F = 26.4 , R = 6%

Run No.	Temp. °C	O_2/N_2	CO_2/N_2	CO/N_2	F_{O_2} mol./sec. x10^6	F_{CO_2} mol./sec. x10^6	F_{CO} mol./sec. x10^6	W/T
18	358	0.2459	0	0	63.926	0	0	0.3279
19	415	0.2373	0	0	61.687	0	0	0.3949
20	470	0.2348	0.0011	0.0023	61.034	0.2792	0.6076	0.4672
21	499	0.2273	0.0021	0.0035	59.074	0.5426	0.9209	0.4907

Run No.	F/T	M/T	F_f mol$_6$/sec. x10^6	F_m mol$_6$/sec. x10^6	T mol$_6$/sec. x10^6	Con. X%	Selct. S%	Yield Y%
18	0.3220	0.3501	9.9742	10.8452	30.9749	47.90	100.0	47.90
19	0.3798	0.2343	12.8590	7.9344	33.8597	61.80	100.0	61.80
20	0.3814	0.1509	13.4855	5.3406	35.3830	73.00	93.83	68.50
21	0.3890	0.1234	14.3019	4.5749	36.7660	77.50	92.80	71.92

Table 8-A-6

W/F = 26.4, R = 8%

Run No.	Temp. °C	O_2/N_2	CO_2/N_2	CO/N_2	F_{O_2} mol./sec. x10^6	F_{CO_2} mol./sec. x10^6	F_{CO} mol./sec. x10^6	W/T
22	358	0.2361	0	0	44.837	0	0	0.3322
23	411	0.2339	0.0007	0.0006	44.430	0.1254	0.1109	0.4121
24	473	0.2304	0.0017	0.0053	43.762	0.3187	1.0040	0.4839
25	499	0.2198	0.0019	0.0049	41.736	0.3648	0.9421	0.4878

Run No.	F/T	M/T	F_f mol./sec. x10^6	F_m mol./sec. x10^6	T mol./sec. x10^6	Con. X%	Selct. S%	Yield Y%
22	0.3293	0.3385	10.3120	10.5978	31.3127	49.32	100.0	49.32
23	0.3755	0.2124	12.7679	7.2222	34.0050	65.30	98.12	64.06
24	0.3838	0.1323	13.9040	4.7915	36.2284	76.10	91.31	69.49
25	0.3960	0.1162	14.6259	4.2930	36.9334	78.80	91.70	72.26

Table 8-A-7

W/F = 26.4, R = 10%

Run No.	Temp. °C	O_2/N_2	CO_2/N_2	CO/N_2	F_{O_2} mol./sec. x10^6	F_{CO_2} mol./sec. x10^6	F_{CO} mol./sec. x10^6	W/T
26	358	0.2285	0	0	34.117	0	0	0.3447
27	410	0.2194	0.0038	0.0023	32.760	0.1217	0.3443	0.4256
28	443	0.2147	0.0020	0.0035	32.056	0.3043	0.5165	0.4576
29	492	0.2106	0.0027	0.0070	31.444	0.4058	1.0434	0.4930

Run No.	F/T	M/T	F_f mol$_6$/sec. x10^6	F_m mol$_6$/sec. x10^6	T mol$_6$/sec. x10^6	Con. X%	Selct. S%	Yield Y%
26	0.3335	0.3219	10.5066	10.1416	31.5073	51.00	100.0	51.00
27	0.3883	0.1860	13.6275	6.5290	35.0942	69.50	96.70	67.20
28	0.3914	0.1511	14.0322	5.4158	35.8537	73.28	94.47	69.23
29	0.3939	0.1131	14.5926	4.1899	37.0430	79.30	90.96	72.16

Table 8-A- 8

W/F =33.4 , R = 6%

Run No.	Temp. °C	O_2/N_2	CO_2/N_2	CO/N_2	F_{O_2} mol./sec. x10^6	F_{CO_2} mol./sec. x10^6	F_{CO} mol./sec. x10^6	W/T
30	329	0.2487	0	0	64.471	0	0	0.3070
31	416	0.2410	0	0	62.645	0	0	0.4445
32	467	0.2360	0.0004	0.0018	61.354	0.1080	0.4581	0.4808
33	505	0.2328	0.0030	0.0030	60.503	0.7762	0.7840	0.5270

Run No.	F/T	M/T	F_f mol$_6$/sec. x10^6	F_m mol$_6$/sec. x10^6	T mol$_6$/sec.. x10^6	Con . X%	Selct. S%	Yield Y%
30	0.3088	0.3833	9.3822	11.6469	30.3839	44.70	100.0	44.70
31	0.3803	0.1752	13.1660	6.0657	34.620.	69.20	96.65	66.88
32	0.4153	0.1040	15.3153	3.8353	36.8821	80.55	96.43	77.60
33	0.4071	0.0658	15.4916	2.5056	40.5580	87.20	90.83	79.20

Table 8-A-9

W/F = 33.4 , R = 8%

Run No.	Temp. °C	O_2/N_2	CO_2/N_2	CO/N_2	F_{O_2} mol./sec. x10^6	F_{CO_2} mol./sec. x10^6	F_{CO} mol./sec. x10^6	W/T
34	332	0.2470	0	0	46.900	0	0	0.3175
35	363	0.2361	0	0	44.802	0	0	0.3924
36	412	0.2230	0	0.0023	42.340	0	0.4294	0.4683
37	463	0.2040	0.0025	0.0053	38.730	0.4706	0.9983	0.5123

Run No.	F/T	M/T	F_f mol$_6$/sec. x10^6	F_m mol$_6$/sec. x10^6	T mol$_6$/sec. x10^6	Con. X%	Selct. S%	Yield Y%
34	0.3089	0.3736	9.3874	11.3515	30.3880	45.20	100.0	45.20
35	0.3758	0.2317	12.6453	7.7972	33.6407	61.85	100.0	61.85
36	0.4041	0.1276	14.5322	4.5880	35.9624	76.50	97.12	74.34
37	0.4077	0.0800	15.4682	3.0355	37.9379	84.80	91.30	77.42

Table 8-A-10

W/F = 33.4, R = 10%

Run No.	Temp. °C	O_2/N_2	CO_2/N_2	CO/N_2	F_{O_2} mol./sec. x10^6	F_{CO_2} mol./sec. x10^6	F_{CO} mol./sec. x10^6	W/T
38	336	0.2319	0	0	34.619	0	0	0.3303
39	362	0.2143	0	0	32.002	0	0	0.3878
40	419	0.2075	0.0004	0.0041	30.980	0.0628	0.6216	0.4874
41	454	0.2031	0.0037	0.0092	30.319	0.5480	1.3778	0.5081
42	482	0.2004	0.0047	0.0096	29.919	0.6996	1.4374	0.5256

Run No.	F/T	M/T	F_f mol$_6$/sec. x10^6	F_m mol$_6$/sec. x10^6	T mol$_6$/sec. x10^6	Con. X%	Selct. S%	Yield Y%
38	0.3152	0.3545	9.7410	10.9561	30.9748	47.50	100.0	47.50
39	0.3812	0.2309	13.0774	7.8718	34.0781	62.43	100.0	62.43
40	0.4266	0.0859	16.1360	3.2489	37.8211	83.80	95.92	80.40
41	0.4289	0.0629	17.2193	2.5280	40.1457	88.34	89.94	79.45
42	0.4298	0.0446	17.4403	1.8092	40.5780	91.55	89.07	81.55

Table 8-A-11

W/F = 42.0 , R = 6%

Run No.	Temp. °C	O_2/N_2	CO_2/N_2	CO/N_2	F_{O_2} mol./sec. x10^6	F_{CO_2} mol./sec. x10^6	F_{CO} mol./sec. x10^6	W/T
43	356	0.2460	0	0	63.916	0	0	0.3875
44	404	0.2329	0.0012	0.0018	60.539	0.3036	0.4601	0.4617
45	458	0.2249	0.0021	0.0035	58.437	0.5366	0.9108	0.5265
46	498	0.2240	0.0025	0.0048	58.198	0.6576	1.2400	0.5305

Run No.	F/T	M/T	F_f mol$_6$/sec. x10^6	F_m mol$_6$/sec. x10^6	T mol$_6$/sec. x10^6	Con. X%	Selct. S%	Yield Y%
43	0.3786	0.2339	12.7952	7.9048	33.7959	61.82	100.0	61.82
44	0.4121	0.1262	15.2579	4.6716	37.0223	77.50	95.20	73.78
45	0.4185	0.0606	16.1523	2.3372	38.6002	88.90	91.80	81.05
46	0.4326	0.0369	17.4612	1.4902	40.3954	93.90	90.20	84.70

Table 8-A-12

W/F = 42.0 R = 8%

Run No.	Temp. °C	O_2/N_2	CO_2/N_2	CO/N_2	F_{O_2} mol./sec. $\times 10^6$	F_{CO_2} mol./sec. $\times 10^6$	F_{CO} mol./sec. $\times 10^6$	W/T
47	356	0.2322	0	0	44.099	0	0	0.3916
48	402	0.2166	0.0015	0.0035	41.132	0.2787	0.6570	0.4799
49	445	0.2128	0.0025	0.0055	40.425	0.4686	1.0399	0.5326
50	496	0.2098	0.0029	0.0093	39.848	0.5533	1.7449	0.5458

Run No.	F/T	M/T	F_f $mol_6/sec.$ $\times 10^6$	F_m $mol_6/sec.$ $\times 10^6$	T $mol_6/sec.$ $\times 10^6$	Con. X%	Selct. S%	Yield Y%
47	0.3779	0.2305	12.7579	7.7823	33.7586	62.11	100.0	62.11
48	0.4315	0.0885	16.6515	3.4166	38.5879	83.75	98.34	82.35
49	0.4211	0.0428	16.3783	1.6660	38.8875	91.50	91.56	83.77
50	0.4213	0.0335	16.9616	1.3486	40.2600	94.46	88.00	83.12

Table 8-A-13

W/F = 42.0 , R = 10%

Run No.	Temp. °C	O_2/N_2	CO_2/N_2	CO/N_2	F_{O_2} mol./sec. x10^6	F_{CO_2} mol./sec. x10^6	F_{CO} mol./sec. x10^6	W/T
51	356	0.2175	0	0.0012	32.477	0	0.1757	0.4037
52	402	0.1970	0	0.0202	29.411	0	0.6762	0.4725
53	470	0.1945	0.0035	0.0139	29.042	0.5220	2.0598	0.5225
54	490	0.1798	0.0932	0.0126	26.852	1.3858	1.9062	0.5785

Run No.	F/T	M/T	F_f mol$_6$/sec. x10^6	F_m mol$_6$/sec. x10^6	T mol$_6$/sec. x10^6	Conv. X%	Selct. S%	Yield Y%
51	0.3941	0.2022	13.7746	7.0678	34.9510	66.40	98.75	66.23
52	0.4510	0.0778	17.8058	3.0707	39.4827	85.76	96.33	82.61
53	0.4089	0.0285	16.3122	1.1302	39.8957	94.60	86.30	81.64
54	0.4061	0.0154	16.6103	0.6309	40.9030	96.93	83.45	80.89

Table 8-A-14

W/F = 48.0 , R = 6%

Run No.	Temp. °C.	O_2/N_2	CO_2/N_2	CO/N_2	F_{O_2} mol./sec. x10^6	F_{CO_2} mol./sec. x10^6	F_{CO} mol./sec. x10^6	W/T
55	345	0.2379	0.0006	0	61.837	0.1567	0	0.4161
56	389	0.2297	0.0004	0	59.701	0.1098	0	0.4682
57	433	0.2210	0.0043	0.0031	57.429	1.1239	0.7967	0.5337
58	482	0.2115	0.0088	0.0060	54.981	2.2788	1.5469	0.5965

Run No.	F/T	M/T	F_f mol$_6$/sec. x10^6	F_m mol$_6$/sec. x10^6	T mol$_6$/sec. x10^6	Con. X%	Selct. S%	Yield Y%
55	0.3696	0.2144	12.4002	7.1943	33.5576	63.60	98.75	62.80
56	0.4321	0.0997	16.0600	3.7069	37.1155	81.86	99.32	81.32
57	0.4315	0.0349	17.3956	1.4054	40.3168	93.30	90.05	83.95
58	0.4023	0	16.6513	0	41.4775	100.0	81.30	81.30

Table 8-A-15

W/F = 48.0 , R = 8%

Run No.	Temp. °C	O_2/N_2	CO_2/N_2	CO/N_2	F_{O_2} mol./sec. x10^6	F_{CO_2} mol./sec. x10^6	F_{CO} mol./sec. x10^6	W/T
59	349.	0.2265	0	0	43.014	0	0	0.4261
60	386.	0.2234	0.0004	0	42.426	0.0812	0	0.4768
61	419	0.2121	0.0017	0.0018	40.270	0.3197	0.3391	0.5094
62	445	0.2054	0.0026	0.0064	38.997	0.4832	1.2072	0.5372
63	470	0.2009	0.0052	0.0080	38.144	0.9879	1.5135	0.5744

Run No.	F/T	M/T	F_f mol$_6$/sec. x10^6	F_m mol$_6$/sec. x10^6	T mol$_6$/sec. x10^6	Con. X%	Selct. S%	Yield Y%
59	0.4108	0.1631	14.7330	5.8490	35.8610	70.15	100.0	70.15
60	0.4438	0.0930	16.8222	3.0098	37.8698	84.90	99.50	84.47
61	0.4576	0.0329	18.2803	1.3134	39.9405	93.52	96.51	90.26
62	0.4563	0.0065	19.0436	0.2719	40.8895	98.71	91.84	90.65
63	0.4256	0	17.4156	0	40.9177	100.0	87.40	87.40

Table 8-A- 16

W/F = 48.0 , R = 10%

Run No.	Temp. °C	O_2/N_2	CO_2/N_2	CO/N_2	F_{O_2} mol./sec. x10^6	F_{CO_2} mol./sec. x10^6	F_{CO} mol./sec. x10^6	W/T
64	372	0.2103	0	0	31.521	0	0	0.4219
65	382	0.2074	0	0	30.960	0	0	0.4582
66	426	0.1980	0.0008	0.0058	29.558	0.1185	0.8715	0.5250
67	452	0.1938	0.0038	0.0015	28.946	0.2810	1.0795	0.5650

Run No.	F/T	M/T	F_f mol./sec. x10^6	F_m mol./sec. x10^6	T mol./sec. x10^6	Con. X%	Selct. S%	Yield Y%
64	0.4418	0.1386	16.6784	5.1700	37.7590	76.60	100.0	76.60
65	0.4444	0.0973	16.8010	3.6778	37.8083	82.00	100.0	82.00
66	0.4531	0.0218	18.2202	0.8776	40.2110	95.60	94.85	90.70
67	0.4350	0	18.2640	0	41.4528	100.0	89.30	89.30

(B) SAMPLE CALCULATIONS

Run No. 57 -

Temperature - 433° C

R/ - 6 %

Gas Analysis -

$(CO / N_2)_h = 0.0137$

$(CO_2 / N_2)_h = 0.0273$

$(O_2 / N_2)_h = 0.3110$

Mole Ratios -

$(CO_2/N_2)_m = 0.225 \times (CO/N_2)_h$

$= 0.0031$

$(CO_2 / N_2)_m = 0.1591 \times (CO_2 / N_2)_h$

$= 0.0043$

$(O_2 / N_2)_m = 0.7157 \times (O_2 / N_2)_h$

$= 0.2221$

As Nitrogen remains unreacted

moles of N_2 in feed = moles of N_2 in product

moles of N_2 in feed = 259.2×10^{-6} moles/sec.

F_{CO} = moles of CO in product

$= 259.2 \times 10^{-6} \times 0.0031$

$= 0.7966 \times 10^{-6}$ moles / sec.

F_{CO_2} = moles of CO_2 in product

$= 259.2 \times 10^{-6} \times 0.0043$

$= 1.1239 \times 10^{-6}$ moles / sec.

F_{O_2} = moles of oxygen unreacted

$= 259.2 \times 10^{-6} \times 0.2221$

$= 57.2130 \times 10^{-6}$ moles / sec.

Liquid Analysis -

Peak height ratios -

$(F/W)_h$ = 1.2793

$(M/W)_h$ = 0.0766

Mole ratios -

$(F/W)_m = 0.632 \times (F/W)_h = 0.8085$

$(M/W)_m = 0.853 \times (M/W)_h = 0.0653$

T is total no. of moles of liquid product

$(F/T) = (F/W)_m \times (W/T)$

$(M/T) = (M/W)_m \times (W/T)$

$T = F_f + F_m + W$

$1 - (W/T) = (F/T) + (M/T)$

$$(W/T) = \frac{1}{1 + (F/W)_m + (M/W)_m} = 0.5337$$

$(F/T) = 0.4315$

$(M/T) = 0.0349$

Material Balance -

M_o = moles of methanol in feed

$$= F_m + F_f + F_{CO_2} + F_{CO} \qquad (8\text{-B-}1)$$

From stoichiometric relationship -

$$W = F_f + 2(F_{CO} + F_{CO_2}) \qquad (8\text{-B-}2)$$

$$T = F_m + W + F_f \qquad (8\text{-B-}3)$$

Placing values of F_m and W from relations 8-B-1 and 8-B-2 in in 8-B-3

$$T = M_o + F_f + F_{CO} + F_{CO_2}$$

$$(F/T) = F_f / (M_o + F_f + F_{CO} + F_{CO_2})$$

$$F_f = (F/T) \times (M_o + F_f + F_{CO} + F_{CO_2})$$

Rearranging -

$$F_f = \frac{(F/T) \times \{M_o + F_{CO} + F_{CO_2}\}}{(1 - (F/T))}$$

$$= 17.3960 \times 10^{-6} \text{ moles /sec.}$$

$$T = 40.3170 \times 10^{-6} \text{ moles /sec.}$$

$$F_m = (M/T) \times T$$

$$= 1.4054 \times 10^{-6} \text{ moles /sec}$$

Carbon balance check -

In feed = 21.0×10^{-6} moles /sec.

In products = $(1.4054 + 17.3960 + 1.2390 + 0.7967) \times 10^{-6}$

$= 20.8371 \times 10^{-6}$ moles/sec.

Error in material balance = 0.1629 moles/sec.

= 0.8%

$$\text{Conversion} = 1 - \frac{1.4054 \times 10^{-6}}{20.8371 \times 10^{-6}}$$

= 93.2 %

$$\text{Selectivity} = F_f / (F_f + F_{CO} + F_{CO_2})$$

= 90.05%

Yield = Selectivity x Conversion

= 83.95%

Material balance check based on Oxygen -

Componeht	Feed in moles/sec. x 10^{-6}	Product moles/sec. x 10^{-6}
CH_3OH	10.50	0.7027
HCHO	0	8.6980
H_2O	0	10.6180
O_2	68.90	57.213
CO	0	0.3983
CO_2	0	1.1239
Total	79.40	78.7544

Errors in material balance of carbon were between -6.8% (Run no. 49) to +4.0% (Run no. 64).

(C) CALIBRATION OF EQUIPMENTS

I. Calibration of Rotameters -

Pressure at outlet of rotameters was kept constant for all runs. Calibration curve for air is given in figure 8-C-1.

II. Calibration of Syringe pump -

Mass flow rate of Methanol = 2.4222 gms/Hr.

Molal flow rate of Methanol = 21.0×10^{-6} moles/sec.

= 0.0756 moles/hr.

III. Calibration of Gas chromatograph and Gas partioner -

Calibration curve for Gas chromatograph is given in figure 8-C-2. Conditions used in chromatograph were -

Carrier gas flow rate = 146.8 cc/min.

Sensitivity = 32.0

Filament current = 150 mA

Temperatures

Column = 100°C

Detector = 115°C

Collector = 100°C

Injector = 200°C

Calibration curve for Gas partioner is given in figure 8-C-3. Conditions used were -

Flow rate of Carrier gas = 89.2 cc/min.

Thermal stablizer set point = 45°C

Filament current = 5 mA

Sensitivity = 10% and 50%

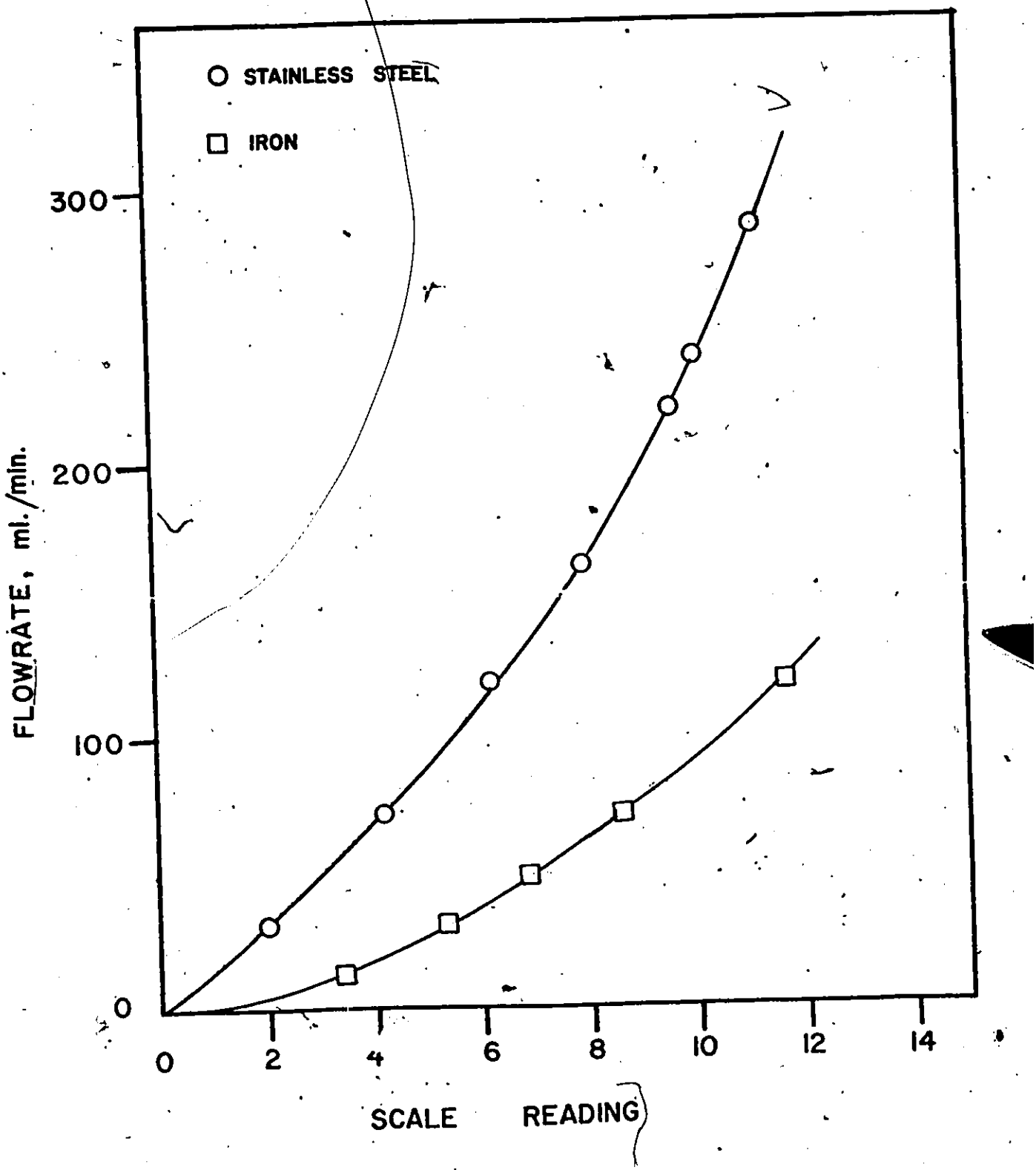

Figure 8-C-1 Calibration curve of Rotameter at T = 22°C and P = 98 cm of Hg

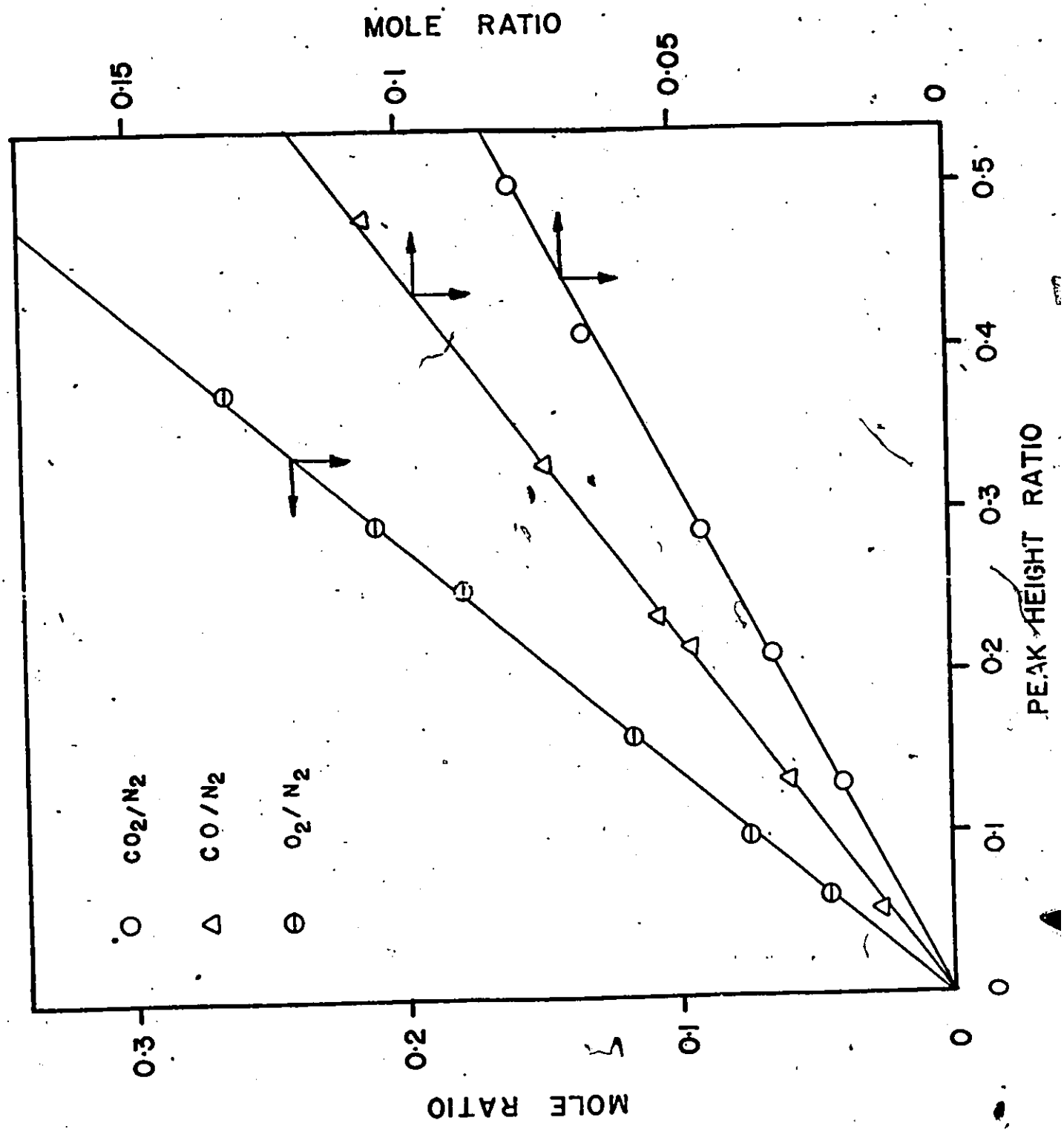
MOLE RATIO
0·15
0·1
0·05
0
0·5
0·4
0·3
0·2
0·1
0
PEAK HEIGHT RATIO
CO_2/N_2
CO/N_2
O_2/N_2
0·3
0·2
0·1
0
MOLE RATIO

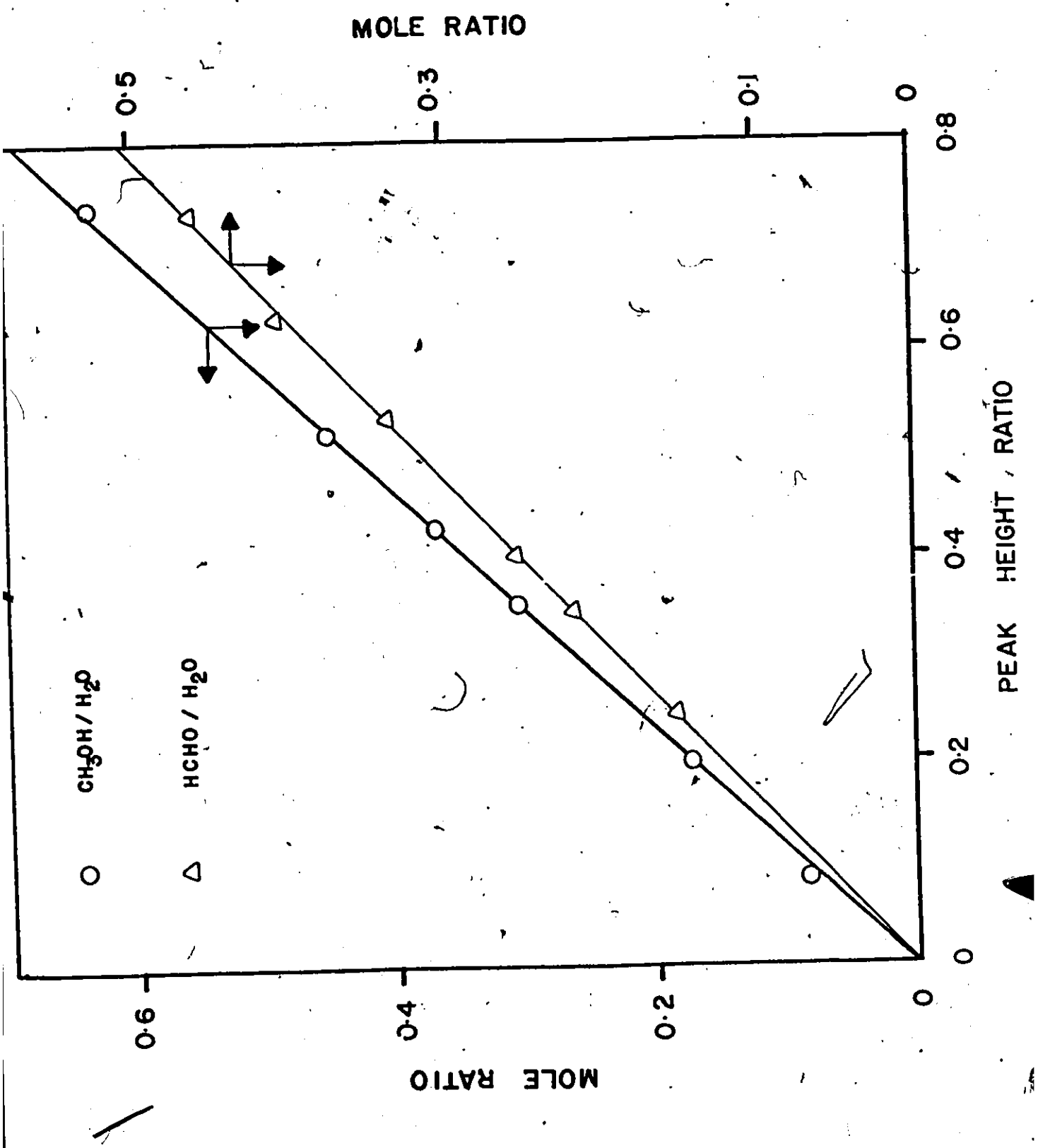
MOLE RATIO
0·5
0·3
0·1
0
0·8
0·6
0·4
0·2
0
PEAK HEIGHT / RATIO
CH3OH / H2O
HCHO / H2O
0·6
0·4
0·2
0
MOLE RATIO

(D) DEVIATION BETWEEN EXPERIMENTAL AND CALCULATED W/F RATIOS

In the table 8-D-1 values of W/F obtained from experimental data are compared with those calculated from final rate expression.

$$\text{Deviation} = \frac{(W/F)_{\text{calculated}} - (W/F)_{\text{experimental}}}{(W/F)_{\text{experimental}}}$$

Values of deviation in general were well within ± 5% except for few runs where conversion was above 90%.

Table 8-D-1

$(W/F)_{exp.}$	R	$(W/F)_{cal.}$ at 380°C	Deviation	$(W/F)_{cal}$ at 430°C	Deviation
13.0	0.08	13.29	2.22%	12.82	-1.38%
26.4	0.08	26.21	-0.72%	26.51	0.40%
33.4	0.08	34.30	2.69%	34.12	2.17%
42.0	0.08	40.22	-4.23%	42.41	0.98%
13.0	0.10	12.45	-4.23%	12.69	-2.41%
26.4	0.10	25.13	-4.80%	25.13	-4.70%
33.4	0.10	31.91	-4.46%	34.41	3.03%

(E) EXTERNAL AND INTERNAL DIFFUSION

(A) External Diffusion -

I .Calculation of pressure drop -

Pressure drop calculations are based on Run no. 37.

W/F = 33.4 Temperature =463° C

Methanol in feed = 8%

Shape factor = 0.9 for irreguler granules

G_m = Molal mass velocity of feed based on catalyst bed

$$= \frac{(241.5 + 21.0) \times 10^{-6} \times 3600}{(\pi/4) \times (2.54 \times 0.390)^2}$$

$$= 1.226 \text{ moles/Hr. cm.}^2$$

a_m = Surface area of catalyst

$= 13100 \text{ cm.}^2 /\text{gm.}$

$(F_j)_{in}$ = Flow rate of component j in the feed

$(F_j)_{out}$ = Flow rate of component j in the product

y_j = mole fraction of component j at the interface

$$= \frac{(y_j)_{in} + (y)_{out}}{2}$$

r_{mj} = Molal reaction rate of component j per unit mass of catalyst

R_j = Dimensionless factor $= r_{mj}/a_m \cdot \phi \cdot G_m$

$$= r_{mj} / 1.444 \times 10^4$$

The values of $(\Delta p_j / p_j)$ were calculated by use of figure -2 of Yoshida et al [51]. These values are listed in table 8-E-1.

Table 8-E-1

Calculation of External Pressure drop

Comp.	$(F_j)_{in}$	$(F_j)_{out}$	$(y_j)_{in}$	$(y_j)_{out}$	y_j	$R_j \times 10^6$	$(R_j/y_j) \times 10^5$	$(\Delta p_j/p_j)_{max.}$
O_2	0.1818	0.1394	0.1931	0.1444	0.1687	1.162	0.689	0.0001
N_2	0.6841	0.6841	0.7266	0.7086	0.7176	0	0	0.0001
CH_3OH	0.0756	0.0109	0.0800	0.0113	0.0456	2.198	4.823	0.0001
HCHO	0	0.0557	0	0.0557	0.0288	1.826	5.289	0.0001
H_2O	0	0.0700	0	0.0725	0.0362	2.380	6.573	0.0001

II . Calculation of temp. drop -

Table 8-E-2

Calculation of Average specific heat of gas

Component	y_j	$(C_p)_j$ Cals. / gm. mole °C	$(C_p)_j \cdot y_j$	Heat of formation K cals. / gm. mole
O_2	0.1087	7.80	1.3159	0
N_2	0.7176	7.26	5.2098	0
CH_3OH	0.0456	16.85	0.7684	-48.0
HCHO	0.0288	11.60	0.3341	-28.29
H_2O	0.0362	8.78	0.3178	-57.80
CO	0.0020	7.56	0.0151	-26.41
CO_2	0.0008	12.32	0.0098	-94.05

$C_{pa} = \sum_{j=1}^{n} C_{pj} \cdot y_j = 7.9709$

ΔH_1 = Heat of reaction for formaldehyde

= -(57.80+28.24) +48.08 . = -38.01

ΔH_2 = Heat of reaction for fomaldehyde conversion to CO

= -(26.41+57.80) +28.29 = -55.92

ΔH_3 = Heat of reaction for formaldehyde conversionto CO_2

= -(94.05 +57.80) +28.29 = -123.56

For one mole of formaldehyde produced 0.05896 moles are further converted to CO and 0.0278 moles are further converted to CO_2.

Molal heat of reaction for one mole of formaldehyde produced-

$$\Delta H = \Delta H_1 + 0.5896 \times \Delta H_2 + 0.0278 \times \Delta H_3$$

$$= -44.74 \text{ K cals./mole} \qquad = -44740 \text{ cals./mole}$$

$$Q_f = \frac{r_{mf} \cdot (-\Delta H)}{a_m \cdot C_p \cdot G_m}$$

$$r_{mf} = 0.02415$$

$$Q_f = \frac{0.02415 \times 44740}{13100 \times 0.9 \times 7.9709 \times 1.226} = 0.00936$$

Maximum pressure drop obtained from figure 4 by Yoshida et al[51] is 0.05°C

B . Internal Diffusion -

Effect of catalyst particle diameter and of changing feed velocity is shown in table 8-E-3.

Table 8-E-3

W/F = 33.4 , Temp. = 454°C , R = 10%

Particle size	Methanol feed rate moles/sec.	Conversion X%	Selectivity S%
60/80 mesh	21.0×10^{-6}	88.34	89.94
40/60 mesh	21.0×10^{-6}	88.16	89.74
60/80 mesh	10.5×10^{-6}	88.50	89.85

(F) RATE CONSTANTS FOR VARIOUS MECHANISMS

The rate constants for other two stage redox mechanisms are listed in tables 8-F-1 to 8-F-4.

Table 8-F-1

Rate constants for m= 1.0 , n = 1.0

Temp. °C	R %	$K_1 \times 10^3$ moles / gm.-mmHg-Hr.	$K_2 \times 10^4$ moles / gm.-mm Hg-Hr.
350	6	0.5822	0.4260
	8	0.7679	0.2263
	10	0.3921	0.4387
380	6	0.7720	0.5329
	8	0.7462	0.4285
	10	0.5254	0.6505
410	6	1.0772	0.5013
	8	1.1119	0.4096
	10	0.8819	0.4947
430	6	1.5597	0.3853
	8	1.5726	0.3635
	10	1.3102	0.4090
450	6	1.3454	0.5457
	8	1.5299	0.4179
	10	1.3807	0.4474
470	6	1.6591	0.4854
	8	1.6872	0.4251
	10	1.6835	0.4313

Table 8-F-2

Rate constants for m = 0.5, n= 0.

Temp. °C	R %	$K_1 \times 10^2$ moles / gm.-mm Hg-Hr.	$K_2 \times 10^2$ moles / gm.-mm Hg. Hr.
350	6	-1.3170	0.1585
	8	10.9248	0.2453
	10	-1.4127	0.1320
380	6	-1.6664	0.2043
	8	-2.7482	0.2193
	10	-1.4838	0.1636
410	6	-2.5654	0.2691
	8	-4.2425	0.2852
	10	-2.7925	0.2397
430	6	-8.9431	0.3723
	8	-12.3419	0.3624
	10	-6.3518	0.3155
450	6	-2.7707	0.3107
	8	-7.7223	0.3643
	10	-7.2582	0.3438
470	6	-3.7697	0.3582
	8	-8.0730	0.3835
	10	-12.3046	0.3896

Table 8-F-3

Rate constants for m=1.0, n=0

Temp. °C	R %	$K_1 \times 10^2$ moles / gm.-mm Hg-Hr.	$K_2 \times 10^3$ moles / gm.-mm Hg-Hr
350	6	3.2836	0.5438
	8	1.3997	0.7690
	10	3.4797	0.3540
380	6	3.2793	0.7810
	8	2.5368	0.7658
	10	4.8610	0.4912
410	6	2.7054	1.1817
	8	2.4891	1.1318
	10	3.1611	0.8462
430	6	2.0172	1.9130
	8	2.1418	1.6591
	10	2.4172	1.3267
450	6	3.4597	1.4440
	8	2.6851	1.4643
	10	2.7711	1.3316
470	6	3.1450	1.6300
	8	2.6956	1.6366
	10	2.6569	1.6228

Table 8-F-4

Rate constants for m = 0.5 , n= 0.5

Temp. °C	R %	$K_1 \times 10^2$ moles / gm.-mm Hg-Hr	$K_2 \times 10^3$ moles / gm.-mm Hg-Hr.
350	6	0.1620	-0.5554
	8	0.2424	5.1613
	10	0.1355	-0.6185
380	6	0.2023	-0.6469
	8	0.2161	-1.0475
	10	0.1664	-0.6316
410	6	0.2603	-0.9138
	8	0.2865	-1.7471
	10	0.2442	-1.2175
430	6	0.3498	-2.2642
	8	0.3638	-5.2000
	10	0.3212	-3.4606
450	6	0.3125	-1.1214
	8	0.3739	-3.7887
	10	0.3526	-3.5211
470	6	0.3646	-2.6100
	8	0.3941	-4.0063
	10	0.4007	-6.8753

Computer Program for Least Square Fit

```
$JOB  ACCT-NUM,SATYEN,TIME=10,PAGES=20
      COMMON/AA/B,B1
      DIMENSIONX(10),Y(10),WBYF(10),CONV(10)
  100 READ(5,10)N,OXM,TOTP
      IF(N.EQ.0)GO TO 120
      WRITE(6,10)N,OXM,TOTP
   10 FORMAT(I10,2F10.3)
      READ(5,11)(WBYF(I),CONV(I),I=1,N)
   11 FORMAT(8F10.3)
      WRITE(6,11)(WBYF(I),CONV(I),I=1,N)
      OXO=(1.0-OXM)*0.788
      OPM=TOTP*OXM
      OPO=TOTP*OXO
      DO 110 I=1,N
      Y(I)=(WBYF(I)/0.5)/CONV(I)
      X(I)=(-ALOG(1.0-CONV(I)))/(0.5*OPM*CONV(I))
      WRITE(6,14)N,Y(I),X(I)
  110 CONTINUE
   14 FORMAT(I10,2F15.6)
      CALL LSTSQ(N,X,Y)
      AK2=1.0/B
      AK1=1.0/B1
      WRITE(6,24)B,B1,AK1,AK2
   24 FORMAT(10X,2E15.6,10X,'AK1=',E15.6,10X,'K2=',E15.6)
      GO TO 100
  120 STOP
      END

      SUBROUTINE  LSTSQ(N,X,Y)
      COMMON/AA/B,B1
      DIMENSION X(10),Y(10)
      X1=0.0
      Y1=0.0
      X2=0.0
      Y2=0.0
        Z=0.0
      DO 110 I=1,N
      X1=X1+X(I)
      Y1=Y1+Y(I)
      X2=X2+X(I)**2.0
      Y2=Y2+Y(I)*Y(I)
      Z=Z+X(I)*Y(I)
  110 CONTINUE
      AN=N
      X3=X1/AN
      Y3=Y1/AN
      S1=X2-X1*X3
      S2=Y2-Y1*Y3
      S=Z-X1*Y3
      B=S/S1
      B1=Y3-B*X3
      S3=S2-B*S
      S4=S3/(AN-2.0)
      WRITE(6,12)N,X3,Y3,B,B1
   12 FORMAT(//5X,'NO. OF POINTS =',I5,5X,'MEAN X =',E13.5,5X,'MEAN Y ='
     1,E13.5/5X,'SLOPE =',E13.5,5X,'Y-ITERCEPT=',E13.5/)
      AMEAN=Y3*Y1
      SLOPE=B*S
      WRITE(6,13)Y2,AMEAN,SLOPE,S3
   13 FORMAT(//5X,'SUM OF SQUARES TOTAL =',E13.5/20 X,'MEAN =',E13.5/'
```

```
     120X,'SLOPE =',E13.5/20 X,'RESIDUAL =',E15.5/)
58         STDX=SQRT(S1/(AN-1.0))
59         STDY=SQRT(S2/(AN-1.0))
60         ERR=SQRT(S4)
61         YBAR=SQRT(S4/AN)
62         STSLP=SQRT(S4/S1)
63         YCPT=SQRT(S4*(1.0/AN+X3**2.0/S1))
64         CRCFT=S/SQRT(S1*S2)
65         WRITE(6,14)
66      14 FORMAT(/5X,'STANDARD DEVIATIONS'/)
67         WRITE(6,15)STDX,STDY,ERR,YBAR,STSLP,YCPT,CRCFT
68      15 FORMAT(/20X,'X=',F10.6/20X,'Y=',F10.6/20X,'ERROR=',E15.5/20X,
        1'Y-BAR=',E15.5/20X,'SLOPE=',E15.5/20X,'Y-INTER=',E15.5/5X,'CORR C
        2OFFICIENT=',F10.6/)
69         RETURN
70         END
   $ENTRY
```

IX. NOMENCLATURE

(g)	Gaseous phase
ΔG	Free energy change
K_1	Rate constant for step 1 of reaction
K_2	Rate constant for step 2 of reaction
K	Rate constant for methanol oxidation
m	Reaction order with respect to methanol
n	Reaction order with respect to oxygen
op_M	Partial pressure of methanol in feed
op_{O_2}	Partial pressure of oxygen in feed
p_M	Partial pressure of methanol at any time t
p_{O_2}	Partial pressure of oxygen at any time t
r	Overall rate of reaction
r_1	Rate of reaction for step 1
r_2	Rate of reaction for step 2
R	Mole % methanol in feed
S	Selectivity
$s_{ox.}$	Oxidized site, active site of lattice or adsorbed oxygen on catalyst
$s_{red.}$	Reduced site of lattice oxygen or the empty site on the catalyst
T	Temperature
W/F	Ratio of weight of catalyst in gms. to methanol feed rate in mol./hr
X	Conversion
Y	Yield of formaldehyde
O_2/N_2	Ratio of moles of Oxygen to moles of Nitrogen in gaseous products
CO_2/N_2	Ratio of moles of CO_2 to moles of N_2 in gaseous products
CO/N_2	Molar ratio of Carbon monoxide and Nitrogen in gaseous products
F_{O_2}	Moles of Oxygen left unreacted per unit time

F_{CO_2}	Moles of Carbon dioxide produced per unit time
F_{CO}	Moles of Carbon monoxide produced per unit time
W/T	Mole% of water in liquid products
F/T	Mole% of formaldehyde in liquid products
M/T	Mole% of methanol in liquid products
T	Total moles of liquid products condensed per unit time
F_f	Moles of formaldehyde produced per unit time
F_m	Moles of methanol produced per unit time

Greek Symbols

θ	Fraction of catalyst surface covered by adsorbed Oxygen
α	Moles of Oxygen required to convert one mole of methanol

All terms used in thecalculation of external pressure and temperature drop in section 8-E have been explained on page 33-35.

X. REFERENCES

1. Walker, J. F; " Formaldehyde", 3rd ed. , Am. Chem. Soc. Monograph Series No. 159, Reinhold Publishing Corporation , N. Y., (1964).

2. Dosi, M. K; M. A. Sc. Thesis , University of Ottawa, Ottawa, (1971).

3. Hahn, K. W; Ph. D.Thesis , University of Ottawa , Ottawa, (1968).

4. Kurina, L. N; and Vorontsova, N. V, Zh. Fiz. Khim., 49(5), 1151-3, (1975).

5. Diem, Hans.; Matthias, Guenther ; and Hussy, Oskar; German Patent No. 2, 220, 665 . (1973)

6. Laidler, K. J; "Chemical Kinetics", 2nd ed. , McGraw-Hill, Toronto p. 5-28, (1965).

7. Obraztsov, A. E.; Shelevich, M. P.; and Popov, B. I.; Zh. Prikl. Khim. (Leningrad), 45(4), 933-4, (1972).

8. Orlova, L. B.; Bobrov, N. N.; and Ione, K. G.; React. Kinet. Catal. Lett., 1(3), 301-6, (1974).

9. Sowards , D. M.; French Patent 2, 021, 164 , (1972).

10. Obraztsov, A. E.; Shelevich, M. P.; and Popov , B. I.; U S S R Patent 321, 009 (1972).

11. Packer, Y; and Davis, B.; J. Chemical Soc., Chemical Communications 19, 803-4, (1974).

12. Adkins, H; and Peterson, W. H.; J. Am. Chem. Soc., 53, 1513, (1931).

13. Courty, Phillipe; and Ajot , Hubert; German Patent 2, 039, 162.

14. Liminov, V. E.; and Varlamov, M. L.; Zh. Prikl. Khim. (leningrad), 43(10), 2261-8, (1970).

15. Hajek, Joroslav; and Zidek , Rudolf; Moravske Chem. Prum., 25(6), 298-9, (1975).

16. Habersberger, K.; and Jiru, P.; Collec. Chzech. Chem. Commun., 37(2), 535-40, (1972).

17. Courty, Phillipe; and Sugier, Andre; German Patent 2,442,311.

18. Pernicone, N.; "Chem. uses of Molybdenum Processing Conf. 1st (1973)," Edited by Mitchell, P. C. H., Climax Molybydenum Co. Ltd., p 155-8.

19. Kowal, L. M.; Muzykantov, V. S; and Kurina, L. N.; Kinet. Katal., 15(5), 1193-7, (1974).

20. Biliznakov, G.; Popov, T.; and Klissurski, D.; Nauch Tr., Plovdivski University Mat., Fiz. Khim. Biol., 11(2), 115-20, (1973).

21. Haas, Hans; Sperber, Heinrich; and Friedrichsen, W.; German Patent 1,932,892.

22. Fedvich, E. V.; and Zhiznevski, V. M.; Khim. Tekhnol. Resp. Mezhved Nauch - Tekh. No. 15, 70-5, (1969).

23. Popov, T. S.; Popov, B. I.; and Bipin, V. N.; U S S R Patent 408,504.

24. Jiru, P; Wicchterlova, B.; and Tichy, J.; Proc. 3rd Cong. of Catalysis North Holland Publishing Co., Amsterdam, p199, (1964).

25. Wichterlova, B.; Jiru, P.; Chem. Prumysl; 15(4), p 198, (1965).

26. Mars, P.; Van Krevelin, D. W.; Chem. Eng. Sc. (Special Supplement on proceedings of the Conference on oxd. process), p41, (1954).

27. Dente, M.; and Collina, A.; Chemica e Industria(Milan), 46, 752 and 915, (1964).

28. Dente, M.; Pasquon, I.; Chemica e Industria(Milan), 47(4), 359, (1967).

29. Klissurski, D. G.; Osn. Pedvideriya Katal. Diestviya Tr. Mezhdunar Kongr. Katal. 4th, (1968), p 374-9.

30. Friedlander, J.; Bennett, C. O.; "Symposium of reaction kinetics in product process design", Am. Inst. Chem. Eng. and Inst. Chem. Eng. Joint meeting in London, p 34, (1965).

31. Cotter, J. T.; Dissertation, University of Rhode Island, Kingston, Rhode Island, (1966).

32. Bliznakov, G.; Jiru, P.; and Klissurski, D.; Collection Czech. Chem. Commun., 31(7), 2995-7, (1966).

33. Boreskov, G. K.; Kolovertnov, G. D.; Kefeli, L. M., Karakchiev, L. G., and Popov, B. I., Kinetika i Kataliz, 7(1), 144, (1966).

34. Popov, A.; Dokl. Akad. Nauk. SSSR, 221(6), 1359-62, (1975).

35. Bliznakov, G.; Popov, T.; and Klissurski, D., Izv. inst. Obshta Neorga. Khim., Bulg. Akad. Nauk., 4, 83, (1966).

36. Arnold, H. R.; U S Patent 2, 320, 253. (1943)

37. Gesmundo, Francesco., Passerone, Alberto., and Rossi Pier, Francesco Rend. Accad. Naz., 40, (1969).

38. Alexe Szabo., Aefred., Rev. Roum. Chim., 15(8), 1197-2000(1970).

39. Popov, T.; Natura (Plavdiv), 3(1), 91-4, (1970).

40. Popov, T.; Natura(Plavdiv), 5(1), 85-90, (1972).

41. Liminov, V. E.; Gooshko, O. N.; Semikina, L. E; Sushchaya, L. E.; and Leleka V. E.; Severodonetsk. Fil.; Gos. Inst. Azotn. Prom., Severodonetsk, Katal. Katal., 9, 41-3, (1972).

42. Hinshelwood, C. N.; "The Kinetics of Chemical Change", Oxford Univ. Press, London, p 207, (1940).

43. Smith, J. M.; "Chemical Engineering Kinetics", 1st ed., McGraw Hill, Newyork, p231-250, (1956).

44. Hougen, O. A.; and Watson, K. M.; "Chemical Process Principles", Part III, McGraw Hill, Newyork, p 824, 834, 929, (1949).

45. Yang, K. H; and Hougen, O. A.; Chem. Eng. Prog., 46, 146, (1950).

46. Morales, M; Spinn, C. W.; and Smith, J. M.; Ind. Eng. Chem., 43, 225, (1951).

47. Schwartz, C. E.; Smith, J. M.; Ind. Eng. Chem., 45, 1209, (1953).

48. Chilton, T. H.; and Colburn, A. P.; Ind. Eng. Chem., 26, 1183, (1935).

49. Gamson, B, W.; Thodes, G.; and Hougen, O. A.; Trans. Am. Inst. Chem. Eng., 39, 1, (1943)

50. Wilke, C. R.; Hougen, O. A.; Trans. Am. Inst. Chem. Eng., 61, 445(1945)

51. Yoshida, F.; Ramaswami, D.; Hougen, O.A.; A.I.Ch. E Journal 8, 5, (1962).

52. Bhattacharya, S.K.; Jankiram, K.; and Ganguly; N.D., J. Catalysis, 8, 128, (1967).

53. Shelstad, K.A.; Downie, J.; and Graydon, W.F.; Can. J. Chem. Eng., 35, 102, (1960).

54. Downie, J.; Shelstad, K.A.; and Graydon, W.F.; Can. J. Chem. Eng., 39, 201, (1961).

55. Ioffe, I.I.; and Lyubarskii, A.G.; Kinetika i Kataliz, 3, 261, (1962).

56. Tarama, K; Teranishi, S.; Yoshida, S.; Tamura, N.; Proc. 3rd Congr. Cataysis (amsterdam), North Holland Publishing Co., Amsterdam, p 283, (1964).

Some of the literature mentioned above is not available in English. This has been referred to through chemical abstracts.